The Thesis Committee for Hao Xin
Certifies that this is the approved version of the following thesis:

Toward Roll-to-roll Transfer of Large-Scale Graphene for Flexible Electronics Fabrication

APPROVED BY
SUPERVISING COMMITTEE:

Supervisor:

Wei Li

Dongmei Chen

Toward Roll-to-roll Transfer of Large-Scale Graphene for Flexible Electronics Fabrication

by

Hao Xin B.S.

Thesis

Presented to the Faculty of the Graduate School of
The University of Texas at Austin
in Partial Fulfillment
of the Requirements
for the Degree of

Master of Science in Engineering

The University of Texas at Austin
December 2013

Acknowledgements

I would like to express my deepest gratitude to my supervisor, Dr. Wei Li for his strong support, invaluable suggestions, and continuous encouragement throughout my research in his group. It is a real honor to be his student. I also want to express my sincere appreciation to Dr. Dongmei Chen who agreed to serve as my thesis reviewer.

I am grateful to Dr. Olivier Bauchau at my undergraduate institution, the University of Michigan-Shanghai Jiao Tong University Joint Institute. He is a great mentor who never fails to enlighten me with his wisdom.

Many thanks to the NASCENT Center, Dr. S.V. Sreenivasan, Dr. Roger Bonnecaze, and other professors and colleagues working at NASCENT. Such a wonderful research opportunity would never happen to me without them.

In addition, I want to thank my friend and colleague Xiaohan Wang for his collaboration regarding graphene characterization and electrochemical delamination. My thesis would not be complete without his help.

Finally, I want to thank my parents for their unconditional love and care from day one.

Abstract

Toward Roll-to-roll Transfer of Large-Scale Graphene for Flexible Electronics Fabrication

by

Hao Xin M. S. E.

The University of Texas at Austin, 2013

Supervisor: Wei Li

Graphene is a promising material for flexible electronics due to its extraordinary electrical, mechanical, and optical properties. One of the biggest challenges today is to transfer large-scale graphene sheet to flexible substrates with minimal quality degradation. In this thesis, a bilayer polymer support for graphene transfer is proposed. Liquid PDMS (polydimethylsiloxane) is first coated on graphene to conform to its surface morphology. A flexible plastic substrate is then pressed on PDMS as a durable support. After PDMS is cured, electrochemical delamination is used to separate graphene from the copper foil. Due to the extremely low work of adhesion between graphene and PDMS, the graphene film on PDMS can be further transferred onto silicon wafer or other flexible substrates by simple adhesion. An added benefit of the PDMS layer is its strain isolation effect, which could protect graphene-based devices from breaking under external loads applied on the flexible substrate. The strain isolation effect of PDMS is verified with an analytical model and finite element analysis. The design of a prototype roll-to-roll graphene transfer machine is also presented.

Table of Contents

List of Tables

List of Figures

Chapter 1 Introduction

1.1 GRAPHENE PROPERTIES

Graphene has received increasing attention in the past decade due to its extraordinary electrical, mechanical, optical, and thermal properties [1-5]. This one-atom thick carbon material was first discovered in 2004 by Andre Geim and Konstantin Novoselov from the University of Manchester when they tried to repeatedly exfoliate graphite with scotch tape. Carbon atoms are patterned hexagonally in a single plane resembling a honeycomb structure (Figure 1.1).

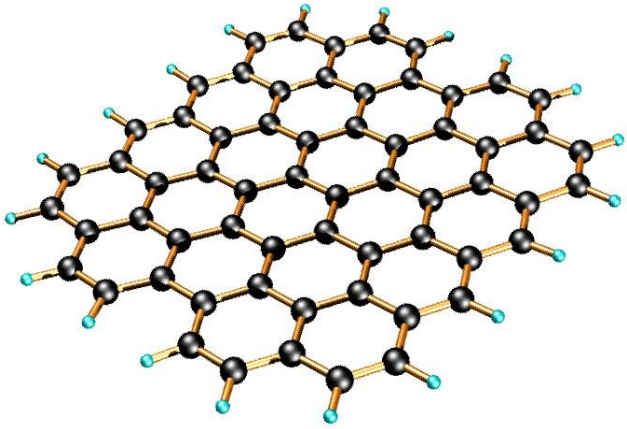

Figure 1.1 Honeycomb structure of monolayer graphene

Picture courtesy: The Tech Journal

An explosion of graphene research followed on the synthesis, transfer, characterization, and electronic device fabrication of this wonder material. Furthermore, research on other 2D materials is motivated by graphene in recent years, such as the dielectric material hexagonal boron nitride and the semiconducting material molybdenum disulfide.

The outstanding mechanical strength of graphene is the result of three strong covalent bonds connecting each carbon atom evenly spaced at an angle of 120 degrees. The Young's modulus of single-layer graphene can be estimated by monitoring the Raman G peak shift when strained is introduced by a pressure difference across the suspended graphene membrane [6]. The result from Raman spectroscopy shows that the intrinsic Young's modulus for monolayer graphene is 2.4±0.4 TPa. Another experimental measurement is carried out with atomic force microscope (AFM) following the same force-displacement relation design, and the Young's modulus of graphene is estimated to be 1.0 ±0.1 TPa [7]. This experimental result by AFM is later verified by a molecular dynamics study, which also claims that the Young's modulus of single-layer graphene increases with increasing sample size until 4 nm when the value reaches a plateau of 1.1TPa [8]. The discrepancy between the two measurements may be due to the different graphene samples used in the experiments. Nevertheless, the terapascal-scale Young's modulus makes graphene one of the strongest materials known today.

Another indicator of the excellent mechanical strength of graphene is the critical strain to cause fracture. It is reported that under a uniaxial stretch test, the fracture strain of monolayer graphene varies significantly from 0.178 to 0.283 due to different chiral angles used in the test (Figures 1.2 and 1.3) [9]. The nominal fracture stress developed in the film ranges from 30.5 N/m to 35.6 N/m, which is more consistent than the fracture strain.

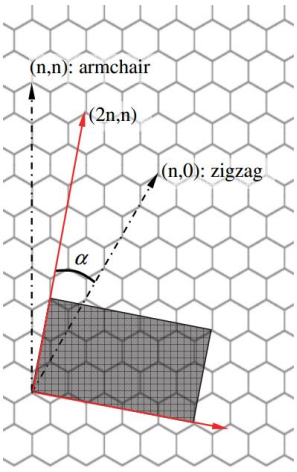

Figure 1.2 Chiral angel α in the graphene hexagonal lattice [9]

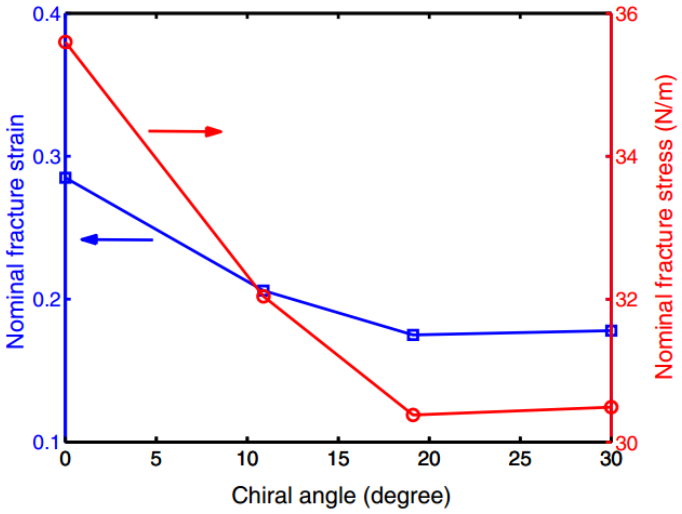

Figure 1.3 Graphene fracture stress and strain variation with chiral angle [9]

However, the previous theoretical prediction is not always applicable since the synthesized graphene films have surface defects and non-negligible roughness so the real fracture strain is lower. According to an atomistic finite bond element model, the defective graphene sheet will start to fracture at the strain slightly below 10%, and it will propagate very fast as the applied strain further increased (Figure 1.4) [10]. Compared

with other inorganic materials used in the semiconductor industry, a fracture strain of 10% is a major improvement.

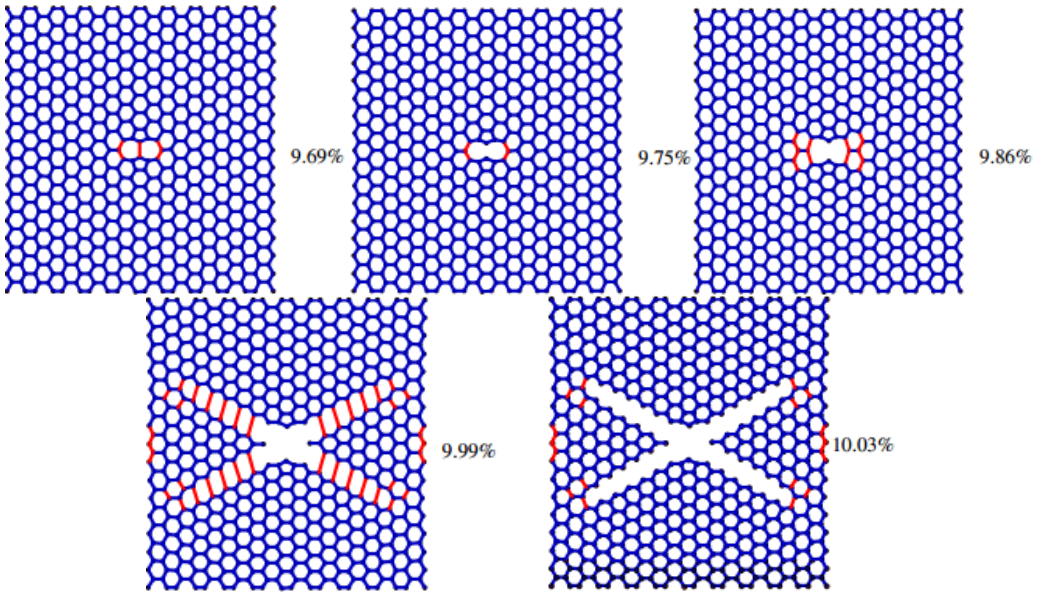

Figure 1.4 Fracture profile of a defective graphene sheet

(The numbers are applied strains) [10]

Graphene is not only well-known for its mechanical properties, but its record-breaking charge carrier mobility and sheet resistance also have sparked extensive research. By suspending a single layer graphene above a Si/SiO_2 gate electrode, researchers at the Columbia University have achieved the electron mobility above 200,000 $cm^2V^{-1}s^{-1}$ at an electron density of $2 \times 10^{-11}cm^{-2}$, which is more than a hundred times higher than that of silicon [11]. In other words, the speed of transistors could potentially increase by at least a hundred times if graphene is used to replace silicon as the base material.

The sheet resistance of the large-scale monolayer graphene film ranges from 125 Ω/sq to 280 Ω/sq [12, 13]. While it is much higher than the sheet resistance of indium tin oxide (ITO), the current material used in transparent electrodes, multiple graphene films can be stacked together to reduce the overall sheet resistance, which is a viable substitute for ITO.

Moreover, monolayer graphene film is highly transparent. It only absorbs 2.3% of the visible light and has a negligible amount of reflection (less than 0.1%) [14]. As a result, large-scale graphene films are suitable for fabricating transparent electrodes since it does not generate glares. Multilayer graphene films with low sheet resistance can still maintain a high optical transmittance to meet the industrial standard for transparent electrodes [15].

1.2 COMMON GRAPHENE SYNTHESIS METHODS

Mechanical exfoliation, epitaxial growth on SiC substrate, and chemical vapor deposition are the three common methods for producing graphene. The quality of the graphene produced and the cost of each method varies significantly.

1.2.1 Mechanical exfoliation

Mechanical exfoliation is the first method used to isolate graphene from bulk graphite. Highly oriented pyrolitic graphite (HOPG) is first attached to a clean scotch tape, and another piece of scotch tape is adhered onto the other side of HOPG. By separating two tapes, the number of graphene layers on each tape is reduced. Same procedure is repeated until monolayer graphene is acquired. Graphene flakes made from

this primitive method usually have extremely small size, irregular shapes, and non-uniform thickness; therefore, they cannot be used to fabricate electronic devices (Figure 1.5) [16]. However, it is worth noting that many studies on graphene properties in the early stage are done with mechanically exfoliated graphene flakes.

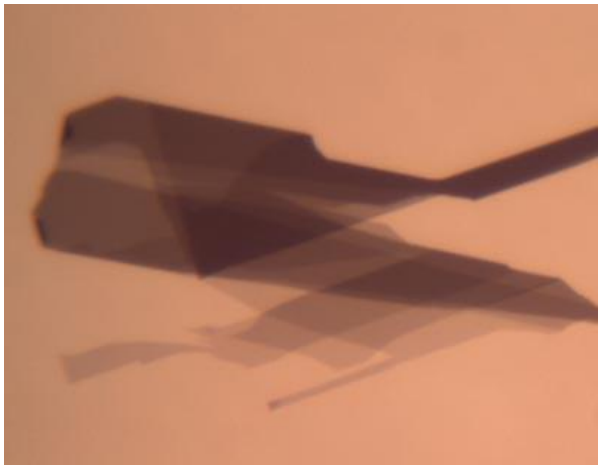

Figure 1.5 Exfoliated graphene on SiO_2/Si wafer

(Graphene is the dark area shown in the picture)

Picture courtesy: Lab of Atomic and Solid State Physics, Cornell University

1.2.2 Epitaxial growth on SiC

Epitaxial graphene growth on SiC is a method to produce large-scale graphene films [17-20]. Silicon carbide (SiC) substrate is heat to 1550 ℃ in a vacuum chamber. Silicon sublimation will take place in a controlled manner leaving carbon atoms on the surface of the SiC substrate to first form an electronically inactive buffer layer (Figure 1.6). Depending on the growth time, monolayer or multilayer graphene film will grow above the buffer layer. However, the high cost of both SiC substrates and the equipment

for creating an ultrahigh vacuum environment prohibits epitaxial graphene growth from large-scale industry application.

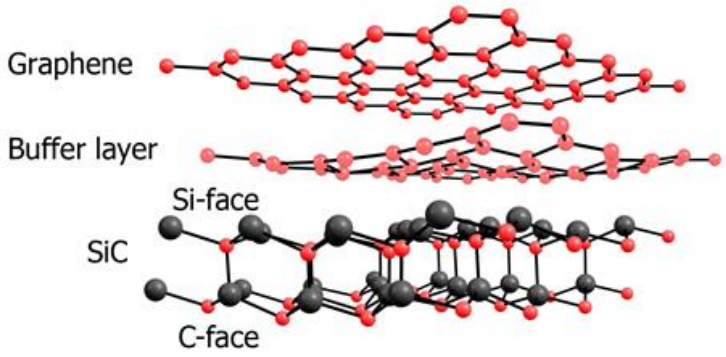

Figure 1.6 Expitaxial graphene growth on SiC substrate

Picture courtesy: University of Groningen

1.2.3 Chemical vapor deposition (CVD)

A cheaper and more efficient way of producing large-scale graphene film is discovered in 2009 through chemical vapor deposition [21]. Copper or nickel foils with a thin oxide layer on top are used as growth substrates. Methane is used as the carbon feedstock, hydrogen is used for oxides and contamination control, and Argon is used as the inert transport gas.

As illustrated in Figure 1.7, the first step is to anneal copper foil in a heating chamber at 1000°C. Since the temperature for annealing is very close to the melting point of copper (1085°C), the copper foil surface will become rough as the residual stress generated during metal forming process being released. Then methane, hydrogen, and argon (optional) are circulated in the chamber for about 10 minutes to allow carbon atoms

to be absorbed by the growth substrate. Next, the chamber slowly cools down to room temperature, and the dissolved carbon atoms will emerge from the surface of the copper foil to form small islands as the result of decreased carbon solubility in copper under lower temperature. Small graphene islands will continue to grow and eventually coalesce to form a continuous graphene film on copper foil [22-24].

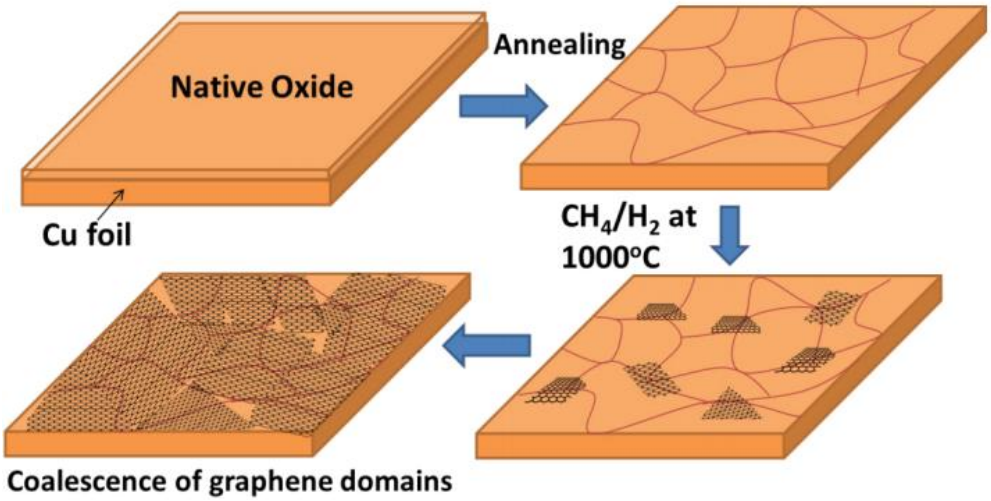

Figure 1.7 Schematic illustration of graphene grown by chemical vapor deposition (CVD) [22]

All the synthesis materials used in chemical vapor deposition are inexpensive and readily available in large quantities. The growth condition is also less stringent than that of epitaxial graphene growth on SiC. Therefore, chemical vapor deposition is by far the most economically viable and reliable method of graphene synthesis which can be scaled up and implemented in the industry.

A roll-to-roll graphene synthesis equipment has been designed to continuous grow few-layer graphene film on copper foil under atmospheric pressure via chemical vapor deposition (Figure 1.8) [25]. Although the quality of the graphene produced from this process is not appropriate for electronics application, but the roll-to-roll design is a good start point for the development of industrial graphene production in the future.

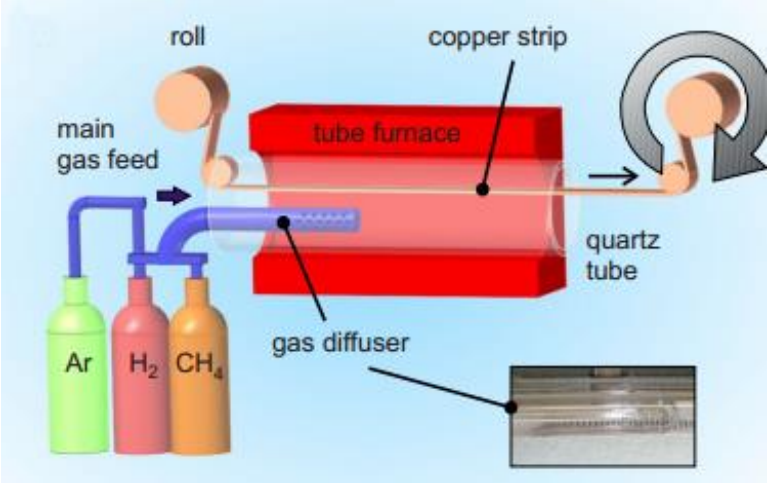

Figure 1.8 Roll-to-roll graphene synthesis by chemical vapor deposition (CVD) [25]

1.3 GRAPHENE TRANSFER

After synthesis on a growth substrate, either copper or nickel film, graphene needs to be transferred onto target substrates for electronics fabrication. It has been experimentally shown that large-scale graphene film with high quality can be synthesized via chemical vapor deposition; however, the quality of transferred graphene often degrades [26]. Cracks and contamination are usually introduced during the graphene transfer process.

Graphene has a large in-plane fracture strain, but the out-of-plane strength is low, and the stepped graphene surface generated during synthesis will also reduce its mechanical strength. In addition, its one-atom thickness also makes the graphene film weak in a macroscopic view. Perturbations encountered as graphene delaminates from copper foil are likely to tear open the localized weak structure of graphene.

Polymer-assisted transfer is commonly used to transfer graphene film from growth substrate to a target substrate. Polymer film or its liquid precursor is first adhered to the graphene film. After curing is complete, copper foil is etched away with an etchant, e.g. ferrous chloride. Then deionized water is used to rinse the graphene film. Finally, graphene is attached to the target substrate and the polymer support is removed by dissolution (Figure 1.9) [27]. Note that some cracks formed during the transfer. During this process, graphene can be contaminated by both copper etchant and polymer residues. As a result, undesirable doping effect will happen, and the carrier mobility of graphene will be reduced [28-30].

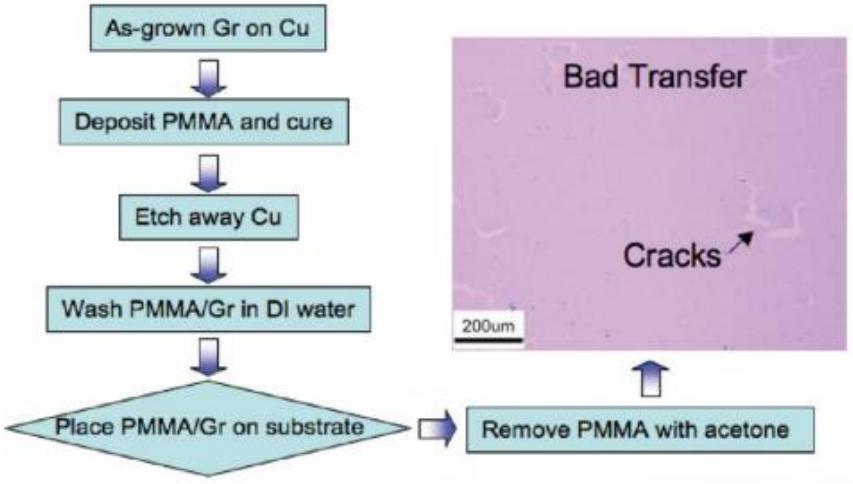

Figure 1.9 Polymer-assisted transfer of CVD graphene [27]

1.4 GRAPHENE-BASED ELECTRONICS

Graphene-based devices are regarded as the potential candidate for post-silicon electronics because of the outstanding electrical properties of this 2D carbon material. Ultra-high speed transistors and flexible transparent electrodes are currently the two most promising products that can be made from graphene.

1.4.1 Flexible transparent electrode

Indium tin oxide (ITO) is the traditional material used for making transparent electrodes; however, it is brittle and will lose its functionality when deformed. ITO is also expensive due to the limited natural resources for indium [31]. As an alternative, graphene has excellent electrical conductivity and high optical transmittance. Most importantly, graphene film can be flexed without compromising its electrical properties. Therefore, graphene-based flexible transparent electrode can be used in touch screens, LCD, OLED, solar panels, and wearable electronics [32-34].

Chemical vapor deposition is usually used to synthesize large-scale continuous graphene film required for making flexible electrodes. The graphene film is then transferred onto flexible substrates, e.g. PET (polyethylene terephthalate), PEN (polyethylene naphthalate), and polyimide. Figure 1.10 illustrates a patterned growth of graphene film with CVD and two possible transfer methods for transparent flexible electrode fabrication [13].

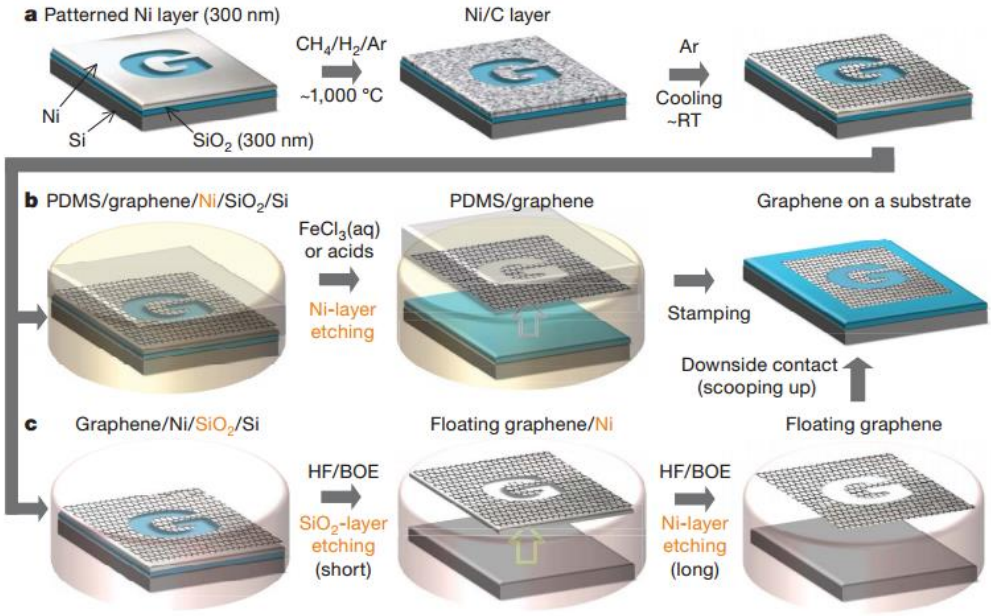

Figure 1.10 Patterned CVD graphene for flexible transparent electrodes [13]

Nickel is used as the growth substrate to grow CVD graphene film. Thick growth substrate will produce graphite crystals instead of graphene due to the large amount of carbon atoms absorbed by the growth substrate under high temperature. Therefore, a 300 nm-thick patterned nickel film is deposited on silicon oxide to ensure a single-layer graphene growth. A standard CVD procedure is carried out and a patterned graphene film is produced on top of the nickel layer.

One way of transferring graphene film to a target substrate is to use PDMS (polydimethylsiloxane) as a backing layer. After adhering PDMS to graphene, nickel layer is etched away, and then graphene on PDMS can be stamped onto PET or any other flexible substrate that has a lower work of adhesion with graphene than PDMS. Another transfer method is to first etch away the silicon oxide layer and then etch away the nickel layer leaving the graphene film floating in the etchant solution. Instead of directly

retrieving it from the solution, the delaminated graphene film is scooped up with the target substrate to protect its integrity.

It is reported that the electrical properties of single-layer graphene transferred on PET film with a PDMS stamp remain stable under uniaxial stretching until the strain developed in the graphene reaches 6% [13]. The researchers also claim that by pre-stretching the polymer flexible substrate, the critical strain for electrical property degradation can be raised to 12%.

One of the major roadblocks for graphene to replace ITO as the new material for transparent electrode is its relatively high sheet resistance. Layers of ITO used in solar cells have a sheet resistance of 10–30 Ω with an optical transmittance around 90% for light of 550 nm wavelength [32, 35]. Even though the intrinsic sheet resistance of a monolayer graphene is around 30 Ω/sq, the value achieved experimentally is much higher [37]. One way to bypass this problem is to stack multiple layers of graphene on top of each other, which could effectively reduce the sheet resistance to the range that is suitable for making transparent electrodes. Furthermore, doping with nitric acid is also shown to be effective in decreasing graphene sheet resistance [37].

As shown in Figure 1.11, the roll-to-roll transferred single-layer graphene has a sheet resistance of 280 Ω/sq. PMMA- assisted graphene transfer with wet etching can produce graphene films with sheet resistance around 140Ω/sq. After doping with nitric acid, the sheet resistance of roll-to-roll transferred graphene decreased significantly to 110 Ω/sq. By stacking four layers of this doped graphene films, the overall sheet resistance can reach the similar level as ITO [37].

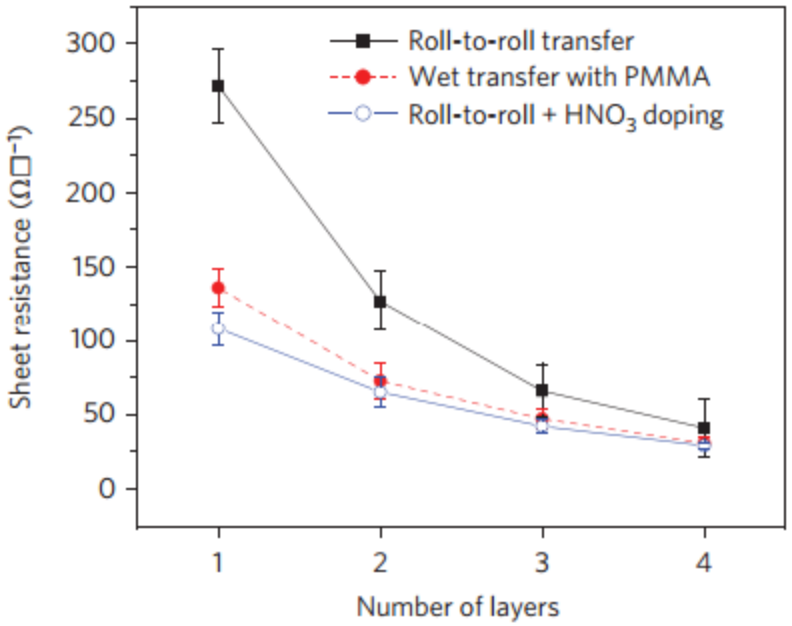

Figure 1.11 Sheet resistances of graphene with different transfer methods [37]

Reaching a low sheet resistance is not the only goal for fabricating transparent electrodes. A high optical transmittance is also necessary to provide a high-quality view for touch screen and display applications. The relation between optical transmittance and sheet resistance of graphene and ITO are shown in Figure 1.12. It can be seen that roll-to-roll transferred graphene films doped with nitric acid has a higher optical transmittance than ITO for the same sheet resistance. Similar results were found by researchers from the Trinity College Dublin that four layers of randomly stacked graphene after doping could achieve a sheet resistance around 10Ω/sq and an optical transmittance of 90% [38]. Hence, by stacking doped graphene films, a flexible transparent electrode can be realized.

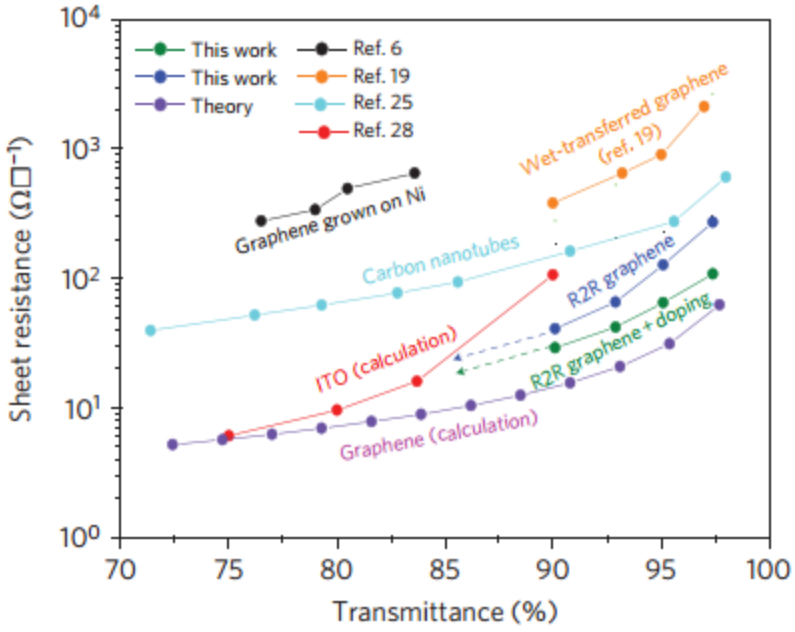

Figure 1.12 Relation between transmittance and sheet resistance of graphene, carbon nanotube, and ITO [37]

1.4.2 Graphene-based transistors

Transistors are used everywhere in modern life, from computers to cell phones and cars. The speed of silicon-based transistors has reached a bottleneck since the resolution of current lithography techniques is limited. Instead of making the device smaller and packing more units on a single chip, another way to improve the transistor speed is to use materials with higher electron mobility. Due to the extremely high electron mobility, graphene is regarded as the material for the next generation of ultrahigh speed transistors [39-41].

The first graphene field effect transistor (FET) was demonstrated by the same research group that discovered graphene in 2004 (Figure 1.13) [1]. The researchers used

few-layer graphene prepared by mechanical exfoliation, which was the only way to acquire graphene at the time. Si/SiO_2 wafer was used as the fabrication platform. The induced electron mobility by applying a gate voltage reached $10{,}000\ cm^2V^{-1}s^{-1}$; however, the overall performance of this preliminary device is not ideal for industrial applications. Nevertheless, it has inspired following research on graphene-based transistors.

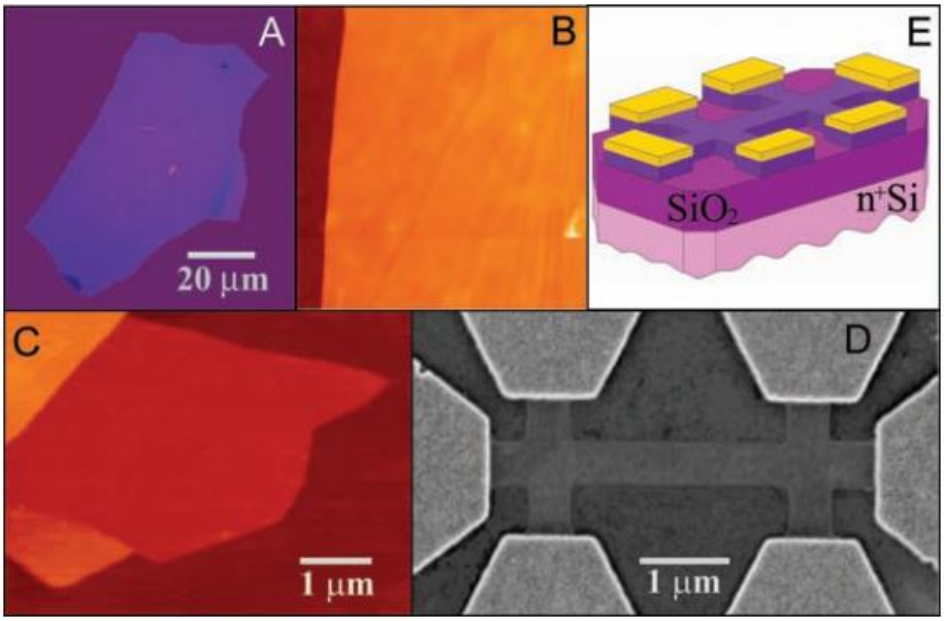

Figure 1.13 First graphene transistor made from few-layer graphene [1]

In 2010, Y. M. Lin et al. reported that the graphene transistors they produced with wafer-scale graphene synthesis and fabrication had a cutoff frequency of 100 GHz (Figure 1.14) [42]. A 2-inch graphene wafer produced via SiC epitaxial growth was used to fabricate transistor arrays with various gate lengths. For a transistor with the gate length of 240 nm, a cutoff frequency was measured to be 100 GHz at a drain bias of 2.5

V. It set a new record for the speed of graphene-based FET when the paper was published. The latest report on graphene transistor from Guanxiong Liu and fellow researchers at the University of California, Riverside claims that the graphene transistor they designed has an operation frequency of 427 GHz, which is already more than a hundred times faster than the state-of-the-art silicon transistor [43].

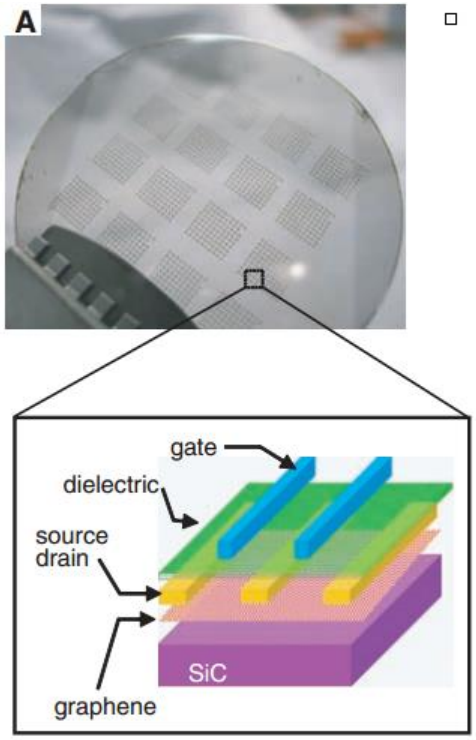

Figure 1.14 Layout of a top-gated graphene field effect transistor [42]

Figure 1.15 illustrates the step-by-step process for fabricating a typical top-gate field effect graphene transistor, which is independent of the wafer size so that this manufacturing technique can be applied to large-scale substrates. First, the conventional photolithography process is used to construct iron catalyst pattern with specified channel

shapes. Second, continuous graphene is grown by chemical vapor deposition on the patterned iron catalyst. Graphene is confined from both sides by the source and drain electrodes made of titanium and gold. Acid is used to etch away the iron catalyst, leaving the graphene film as a bridge between the two electrodes. Next, a layer of hafnium dioxide is deposited around the graphene film as a back-up layer using atomic-layer deposition. Finally, the gate is embedded on top of the graphene film with the hafnium dioxide coating, and the transistor is complete. Even though difference in materials and structures are seen in other top-gate graphene field effect transistor fabrication methods, the main process flow and fabrication techniques are transferrable.

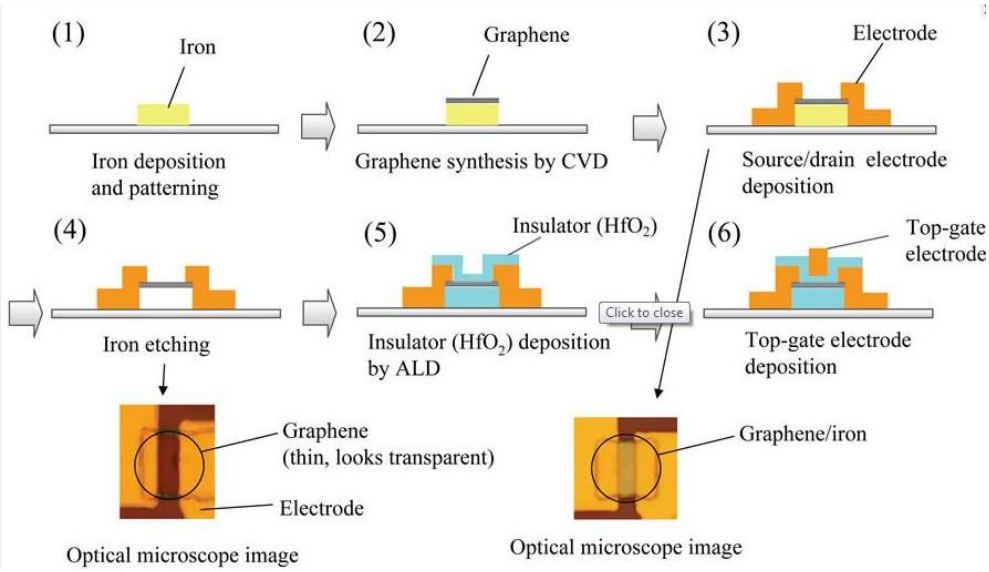

Figure 1.15 Illustration of top-gate field effect graphene transistor fabrication

Picture courtesy: Fujitsu

One major challenge in graphene-based transistors is the low on/off resistance ratio which is induced by the lacking of bandgap in graphene. The absence of the

saturation region in the output characteristics also makes graphene infeasible to be used for logic operations [44]. However, the ultrahigh carrier mobility together with its nanoscale length will gives graphene-based transistors great potential in analog circuits and radio frequency communications [45, 46].

1.5 RESEARCH MOTIVATION AND OBJECTIVES

Graphene has great potential in the post-silicon electronics industry. Field effect transistors made from graphene is a hundred times faster than the silicon-based counterpart, and the graphene transparent electrode can maintain its functionality under large deformation. Graphene films synthesized via chemical vapor deposition have the required mechanical, electrical, and optical properties for large-scale industrial application in flexible electronic devices. However, the quality of CVD graphene usually degrades during the transfer process. Therefore, a reliable and efficient roll-to-roll graphene transfer process is urgently needed to realize the potential of graphene in the next generation electronic devices.

1.6 PROPOSED METHOD

PDMS and a flexible plastic film are used to achieve a clean and high-quality transfer of CVD graphene from the growth substrate. The transferred graphene film on PDMS and plastic film can be directly used to fabricate flexible electronics. One benefit of this structure is that PDMS could effectively shield graphene from externally applied loads. In addition, graphene on PDMS can be further transferred onto other target substrates due to the low work of adhesion between graphene and PDMS. Instead of wet etching of the growth substrate, electrochemical delamination is used to separate the

graphene film from its metal foil growth substrate, so that the metal foil can be reused. Experiments were conducted to demonstrate the feasibility of this proposed transfer process. The design of a roll-to-roll transfer machine was evaluated to implement the proposed graphene transfer scheme.

1.7 THESIS ORGANIZATION

The properties of graphene and the potential of graphene-based electronics are introduced in Chapter 1. Three common methods to acquire this material are reviewed: mechanical exfoliation, epitaxial growth on SiC, and chemical vapor deposition. Graphene transfer as a necessary step from synthesis to device fabrication is also briefly discussed. Field effect transistors and flexible transparent electrodes are selected as examples to illustrate the potential of graphene in the electronics industry.

In Chapter 2, four different polymer-assisted graphene transfer methods with PMMA, PDMS, thermal release tape, and silicone/PET are critically reviewed. In addition, review on inorganic electronic device protection is conducted to compare with graphene-based devices.

In Chapter 3, a new graphene transfer process is demonstrated with PDMS and a plastic backing layer using electrochemical delamination. The quality of transferred graphene film is compared with that of other common graphene transfer methods. The preliminary experiments conducted that lead to this final bilayer polymer support are also explained in detail in the beginning of this chapter.

In Chapter 4, the strain isolation effect of the intermediate PDMS layer between graphene and plastic film is analyzed. Comparison is made with similar techniques reported for inorganic electronics protection. An analytical model, as well as a finite element analysis, is carried out to demonstrate the effectiveness of this PDMS buffer layer.

Chapter 5 discusses the roll-to-roll graphene transfer machine design and preliminary concepts to realize the proposed graphene transfer process. Several 3D models are generated to evaluate the conceptual designs.

Finally, Chapter 6 summarizes the results of this research and provides recommendations for future work.

Chapter 2 Literature Review

2.1 POLYMER-ASSISTED GRAPHENE TRANSFER

In most cases, the growth substrate of graphene is not used as the final substrate for device fabrication, so a transfer process is required to safely separate the graphene film from its growth substrate and attach it to the target substrate. The current graphene transfer methods fall into two major categories, direct mechanical delamination, and polymer-assisted transfer [47].

Graphene is first discovered by mechanical delamination from bulk graphite with scotch tape. Highly oriented pyrolic graphite (HOPG) is used since graphene exfoliated from HOPG has a well-ordered crystalline structure [48-50]. However, the graphene flakes produced in this hash peeling process usually have varying shape, size, and thickness.

When chemical vapor depostition is employed to synthesize graphene on metal foils, polymer-assisted transfer methods are developed for CVD graphene films. Polymer film or its liquid precursor is first coated on as-grown graphene, and the graphene growth substrate is subsequently etched away with proper metal etchant. Graphene on the polymer support is then transferred onto the target substrate after being cleaned with deionized water. Finally, polymer backing layer is removed with organic solvent or direct peeling.

Compared with mechanical exfoliation, polymer-assisted graphene transfer can produce much larger graphene sheet with high quality. Common polymers used for

graphene transfer are PMMA, PDMS, thermal release tape (TRT), epoxy, polyimide etc [47, 51-55].

2.1.1 Graphene transfer with PMMA

PMMA (polymethylmethacrylate) is the most widely used polymer for graphene wet transfer, and this technique was inspired by the similar use of PMMA to transfer carbon nanotube films [56]. PMMA-assisted transfer method is first used to transfer mechanically exfoliated graphene flakes onto Si/SiO_2 wafer (Figure 2.1) [57]. Few-layer graphene flakes are produced from HOPG and attached to Si/SiO_2 wafer when graphene is first discovered.

In addition, graphene on Si/SiO_2 wafer can be further transferred onto a new substrate. First, liquid PMMA precursor is evenly spread on graphene film by spin coating, and the thickness of PMMA film is adjustable by controlling the time and speed of spin coating. Curing is followed and covalent bonds are formed between PMMA and graphene. Next, silicon oxide is etched away with sodium hydroxide and graphene is freed. Graphene is attached to the target substrate and acetone is used to wash off PMMA backing layer. Deionized water is used to rinse the transferred graphene on target substrate. Similar procedure is used to transfer large continuous graphene film synthesized by chemical vapor deposition, and the only difference is the growth substrate as well as the corresponding metal etchant required.

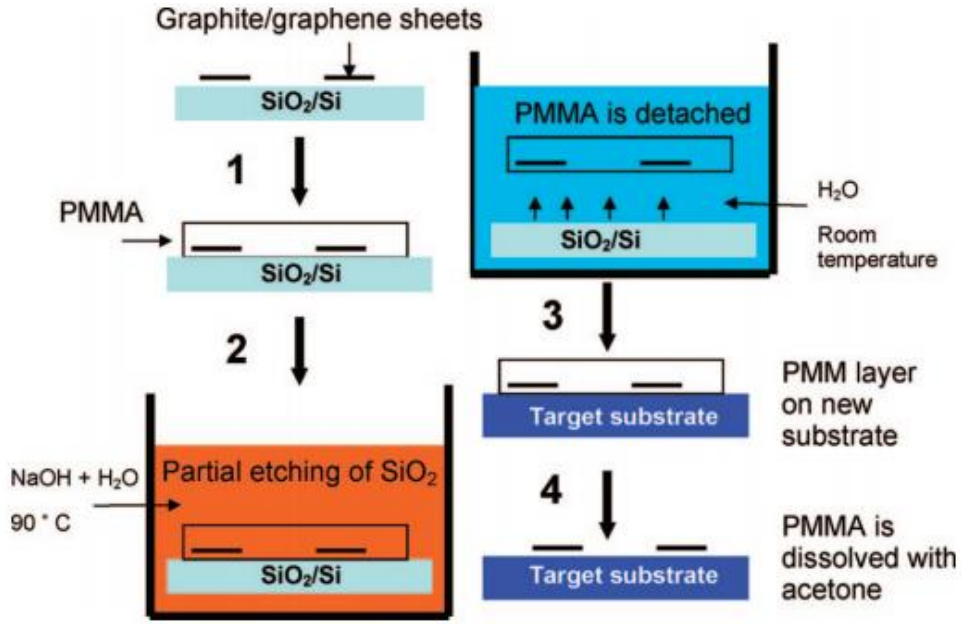

Figure 2.1 Illustration of PMMA-assisted graphene transfer for graphene flakes [57]

The Ruoff group from the University of Texas at Austin suggested a so-called PMMA reflow method to improve transferred graphene quality when PMMA is used as polymer backing layer (Figure 2.2) [27]. It is reported that cured PMMA is rigid and will keep the wrinkles in graphene film generated during chemical vapor deposition. When graphene is attached to the target substrate, the relatively rough graphene surface is incompatible with the smooth surface of the target substrate. Gaps will form in the defetive zone and graphene film could be potentially washed off during PMMA removal stage. By redopsiting liquid PMMA on top of the cured PMMA film, the strain developed in graphene can be relaxed and a conformal contact between grapehen and the target substrate is realized.

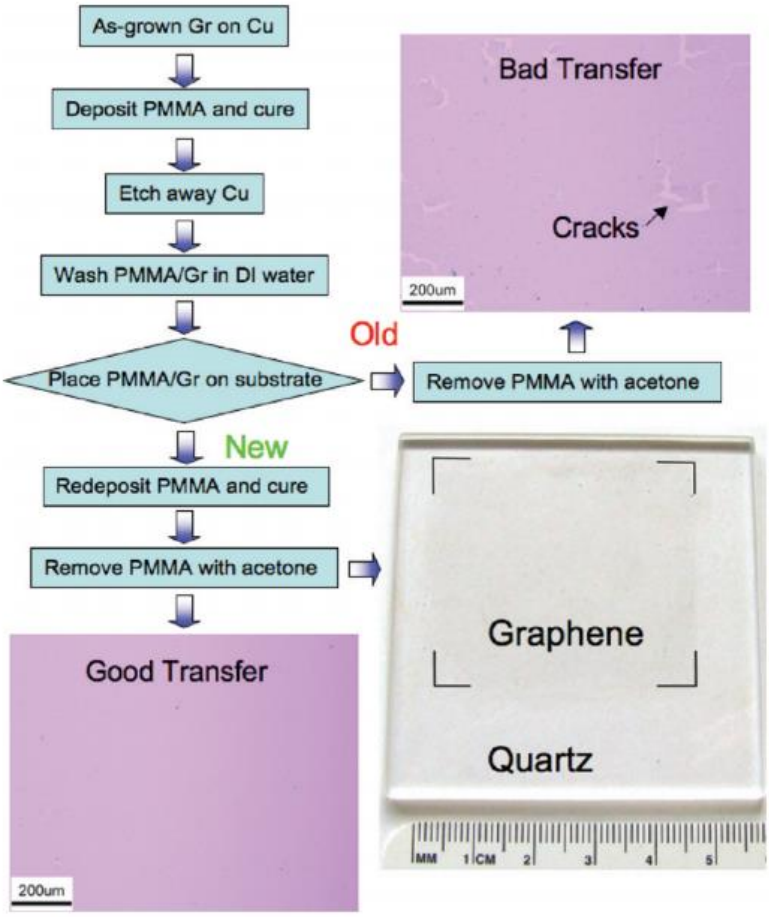

Figure 2.2 Conformal graphene contact achieved with PMMA reflow [27]

2.1.2 Graphene transfer with PDMS

PDMS (polydimethylsiloxane) is another popular polymer used as the support layer in graphene transfer. PDMS is a durable rubberlike material commonly applied in the field of soft lithography [58]. One benefit of PMDS is its extremely low surface energy [59]. Graphene on PDMS can be readily transferred to almost any target substrate, whether rigid or flexible, and then PDMS can be simply peeled off without compromising graphene integrity. Sometime, PDMS-assisted graphene transfer is also

referred to as “graphene stamping”. It has been demonstrated that pre-patterned PDMS stamp can be used to transfer CVD graphene for device fabrication (Figure 2.3) [60].

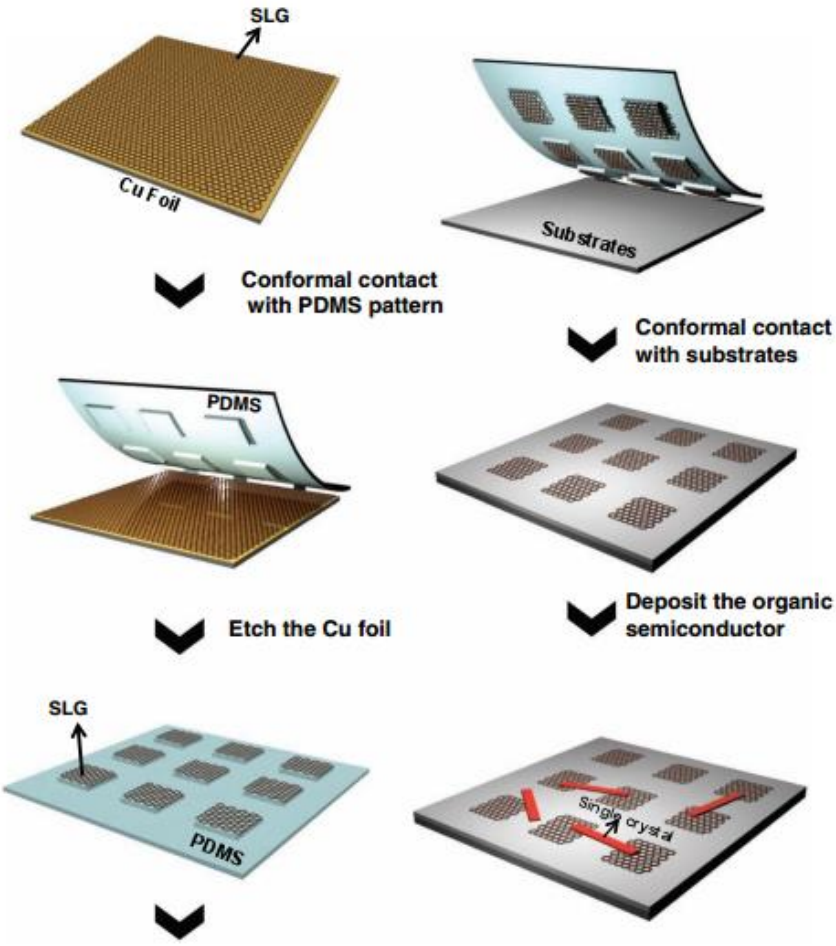

Figure 2.3 Graphene transfer and patterning with PDMS stamp [60]

As illustrated in Figure 2.3, PDMS stamp is patterned with desirable geometry and pressed onto a continuous CVD graphene film on copper foil. During the metal etching process, only the graphene that adhered to PDMS stamp is preserved. Next, the patterned graphene on PDMS is stamped onto the target substrate and PDMS support is

released. High-performance organic field effect transistors are fabricated with graphene as its source and drain electrodes, which has an on/off current ratio of $\sim 10^7$ and a field effect mobility of $\sim 10\ cm^2/Vs$ [60].

2.1.3 Graphene transfer with thermal release tape (TRT)

The use of thermal release tape as backing layer for graphene transfer is first reported by Caldwell et al. in 2009 to dry transfer epitaxial graphene onto SiO_2, GaN, and Al_2O_3 substrates with relatively low graphene quality degradation [55]. The successful graphene transfer with TRT has inspired a roll-to-roll continuous transfer of graphene from copper foil (Figure 2.4), and more graphene transfers with TRT as polymer support are reported [37, 61-63].

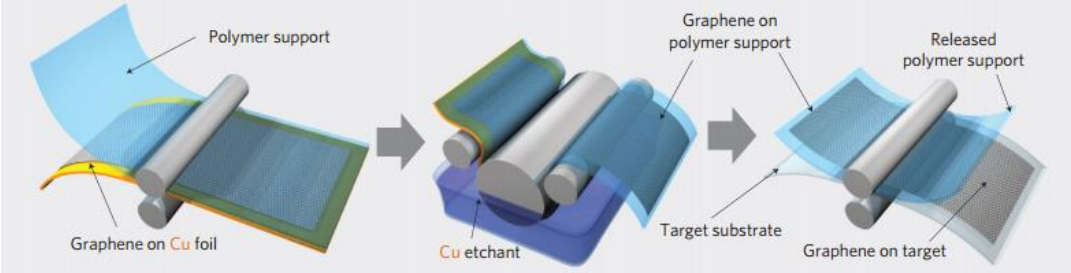

Figure 2.4 Roll-to-roll graphene transfer with thermal release tape [60]

Graphene films transferred with TRT are used to make top-laminated graphene electrode in solar cells (Figure 2.5) [64]. Multiple layers of graphene films are stacked by repeated transfer of CVD graphene from copper foil. The performance of the resulting solar cell has reached 76% of the solar power conversion efficiency of standard commercial solar cells with silver electrodes.

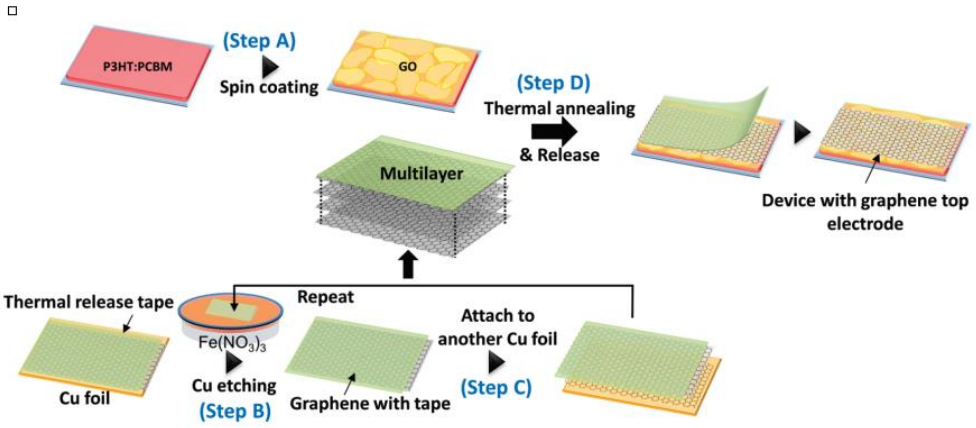

Figure 2.5 Repeated graphene transfer with thermal release tape [64]

The thermal release tape used for graphene transfer is manufactured by Nitto Denko. TRT can temporarily adhere to graphene at room temperature, and it can be released when the critical surface temperature of the film is reached. Figure 2.6 shows the adhesive strength of TRT as a function of its surface temperature. The critical temperature for release can be adjusted for specific application by changing the adhesive composition.

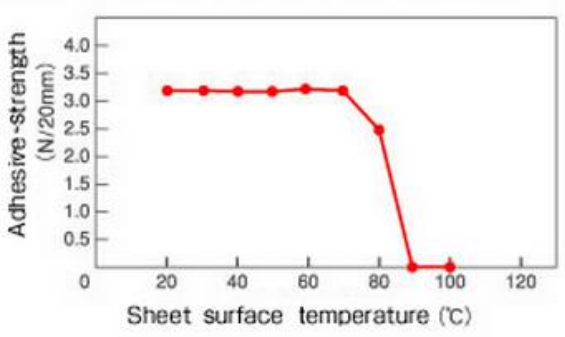

Figure 2.6 Temperature-dependent adhesive strength of thermal release tape

Picture courtesy: Nitto Denko Corp.

2.1.4 Graphene transfer with silicone/PET

A two-layer structure composed of silicone and PET film is also used as the transfer support layer, which has reportedly achieved a clean and efficient transfer of large-area CVD graphene onto different substrates (Figure 2.6) [65]. The researchers claim that the dispersive adhesion mechanism between silicone and graphene will not result in any polymer residues on transferred graphene film.

A commercial screen protector for smartphones is used in the experiment as the silicone/PET support layer. This bilayer film is first pressed onto graphene with a pressure of 50 kPa for one hour. Glass slides are used on both sides to ensure a uniform applied pressure. Wet etching is used to remove the copper growth substrate, and HCl is used to clean up residual Fe^{-3} ions on the graphene surface. In the last step, graphene is transferred on the target substrate and silicone/PET film is peeled off. Like graphene transfer with TRT, the silicone/PET transfer method can also be scaled up and implemented in a continuous roll-to-roll design.

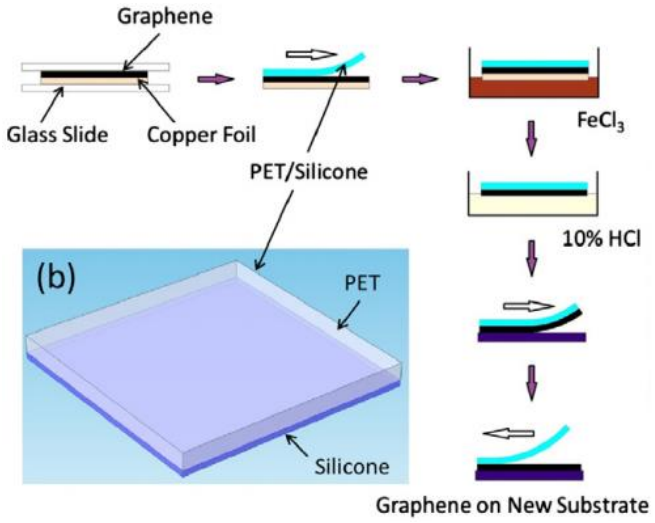

Figure 2.7 Clean transfer of CVD graphene with silicone/PET [65]

2.2 INORGANIC DEVICE PROTECTION WITH ELASTOMERS

Foldable and stretchable electronics are envisioned by many as the future development trend for portable devices and high-resolution displays. This rising research interest has been reported in the past decade around the globe, and one major thrust in this area is the hybrid design of both soft materials and hard materials. Silicon-based materials are still dominant in today's semiconductor industry. They are hard, brittle, and prone to cracks under small deformation. To integrate these traditional brittle metals in flexible electronics, soft material like elastomers are used to as the strain isolation shield for inorganic devices embedded in them (Figure 2.8) [66-68].

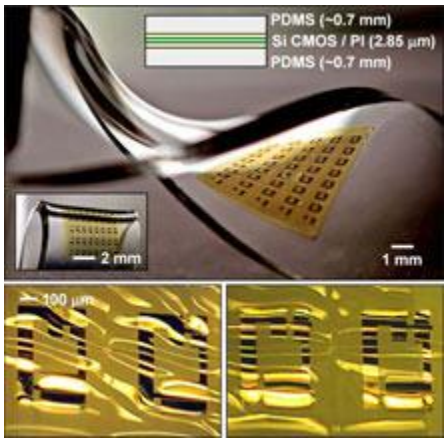

Figure 2.8 Silicon electronics embedded in elastomers

Picture courtesy: MIT Technology Review

John Rogers and the researchers in his group at UIUC are the leading experts in the area of inorganic devices protection with elastomers. They have successfully demonstrated that devices made from highly brittle metallic materials with proper elastomer shielding will maintain its functionality under large external loads [69-73]. PDMS is an ideal choice for the strain isolation layer, which could effectively increase

the critical fracture strain for inorganic devices on flexible substrates by more than a hundred times [69]. Multiple layers of silicon-based circuits can be stacked in PDMS that could survive a bending radius of 400 μm (Figure 2.9) [70].

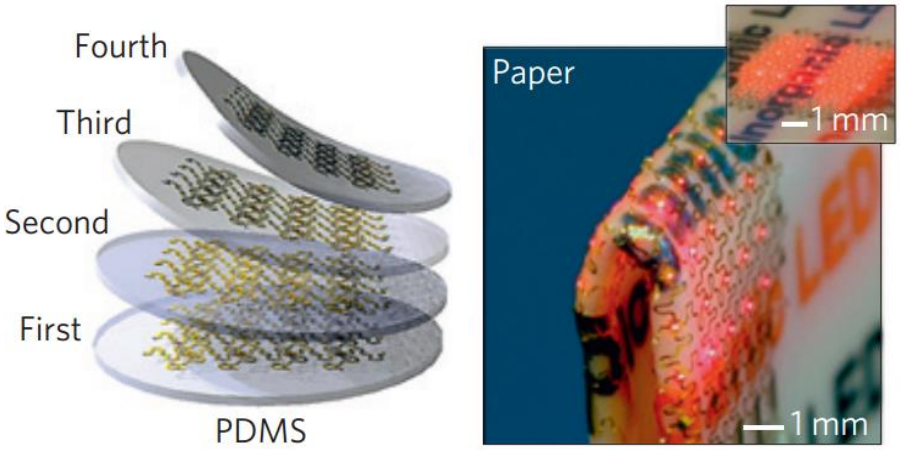

Figure 2.9 Multi-layer circuits bent with small radius [70]

There is a wide range of applications for this hybrid circuit design. One example is biomedical electronics shielded by biocompatible elastomers. With the strain isolation effect, medical monitoring and regulating devices could be safely implanted into human body and remain functional under large change in its geometry (Figure 2.10) [71].

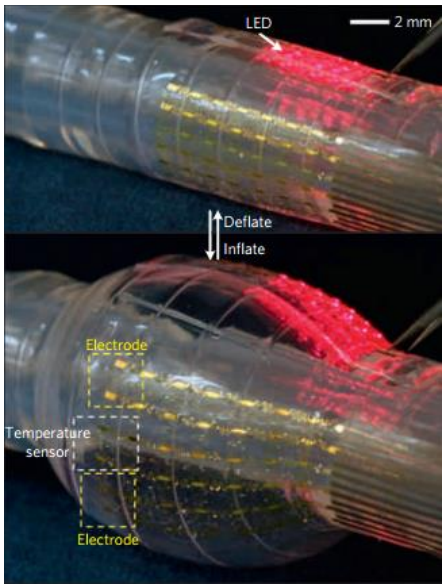

Figure 2.10 Inflatable balloon catheter with strain isolation design [71]

Chapter 3 Graphene Transfer with PDMS/Plastic and Electrolysis

3.1 INTRODUCTION

Graphene has received increasing attention due to its high electrical conductivity, flexibility, and excellent optical transmittance [1-5]. All of the three properties are desirable for flexible electronics designs, such as field effect transistors, light emitting diodes, and transparent conductive electrodes for touch screens [13, 27, 74, 75].

To date, chemical vapor deposition (CVD) with copper or nickel foil as the catalytic growth substrate has been a preferred method for producing large-scale single-layer graphene films with high quality [21-24]. Compared with epitaxial graphene growth on SiC substrate, the large bendable copper foil can be used as the growth substrate that can be later implemented into a roll-to-roll transfer process [37]. Degradation of graphene quality usually happens during the transfer process, so the challenge remains in how to transfer graphene film grown on copper foil to target substrates, e.g. PET, PI, or other polymer films with minimal tears, corrugations, and contamination [27, 76].

In this chapter, a bilayer transfer support is introduced to achieve a high-quality large-area graphene transfer from its growth substrate to various target substrates with the final goal of roll-to-roll graphene transfer implementation. Degased PDMS (polydimethylsiloxane) precursor is used to form conformal contact with the stepped graphene surface, and a plastic film is pressed on the uncured PDMS to act as a rigid transparent backing layer. The plastic film can be PET, PEN, Kapton (a polyimide film developed by DuPont), or any other film that can provide rigid support. After PDMS is cured, copper foil can be either etched away with aqueous ferric nitrate solution, or

electrolysis can be used to separate graphene from copper foil by forming hydrogen bubbles in between [78-80]. The advantage of using electrochemical delamination is that the copper foils can be recycled and no chemical doping will be caused by the copper etchant.

The graphene/PDMS/hard plastic film itself is an excellent candidate for flexible electronics patterning since PDMS is extensively used in soft lithography [81]. Moreover, the graphene film on PDMS can be further transferred onto a rigid substrate (e.g. silicon oxide) or a flexible substrate (e.g. PET film). Unlike the strong covalent bond between PMMA and graphene, PDMS adheres to graphene through dispersive adhesion, an adhesion mechanism that only involves intermolecular interactions between two materials that are brought close to each other [65]. Therefore, the work of adhesion between graphene and PDMS is so low that the graphene film can be transferred to almost any substrate by uniformly pressing against the target substrate and peeling off the PDMS layer after thorough adhesion [13, 59]. No residue is left on the transferred graphene film because of the weak bonding of the dispersive adhesion between PDMS and graphene.

3.2 PROPOSED GRAPHENE TRANSFER METHOD

To acquire high-quality large-scale graphene film on flexible substrates for device fabrication, proper polymer backing layer and safe delamination technique are essential. In this chapter, a double-layer structure consisting of PDMS and PET film is proposed. In addition, electrochemical delamination is used to separate graphene from its growth substrate so that the metal foil can be recycled. Multiple experiments are carried out that

lead to the final design of the bilayer layer support. From the transferred graphene quality, it is found that liquid PDMS is better than cured PDMS film and a relatively rigid PET film can provide necessary support to the soft PDMS layer.

3.2.1 Overview of polymer-assisted graphene transfer methods

Polymer-supported etching and transfer are mainly developed to facilitate CVD-grown graphene transfer, and PMMA (polymethylmethacrylate) is one of the widely used polymer supports. Liquid precursor of PMMA is spin coated on graphene film and cures under elevated temperature. Copper foil is then etched away, leaving graphene on cured PMMA layer. Finally, graphene film is attached to the target substrate and PMMA is dissolved away by acetone [24]. There are several disadvantages associated with the PMMA-assisted graphene transfer. First, the low mechanical strength of PMMA renders large-scale graphene transfer impractical [24, 27]. Second, PMMA forms covalent bonds with graphene after curing and this strong adhesion force may induce cracks when transferring graphene to the target substrate [47]. In addition, PMMA cannot be completely washed away by acetone, and the residues will cause p-type doping and carrier scattering of the transferred graphene film [29].

Another recently reported intermediate support layer for graphene transfer is the thermal release tape (TRT) developed by Nitto Denko Corp. The transfer process with TRT is similar to PMMA-assisted transfer with the exception that TRT instantly adheres to graphene film and readily releases from graphene onto the target substrate when adequate heat is applied [37, 51, 77]. Using TRT as the support layer, Bae, Sukang, et al. demonstrated a roll-to-roll transfer of a 30-inch graphene film, and they successfully built

a flexible touch-screen panel with multilayered graphene films stacked on a PET substrate by this roll-to-roll transfer. Nevertheless, TRT inevitably introduces residue upon removal which appreciably degrades graphene quality and the solution to which has not been found [37, 47].

Therefore, a support structure that can achieve clean and roll-to-roll compatible graphene transfer is needed for flexible electronics fabrication.

3.2.2 Design of polymer backing layer

Inspired by the silicone/PET bilayer support design [65], a verification experiment is done with a commercial screen protector. Electrochemical delamination is used after the polymer support is attached to graphene on copper foil (Figure 3.1).

Figure 3.1 Graphene transfer with silicone/PET and electrochemical delamination

The transferred graphene on silicone/PET is characterized with optical microscope and Raman spectroscopy (Figure 3.2). It can be seen that cracks are formed in the graphene sheet during the transfer process. The high 2D/G ratio indicates that the graphene on silicone is monolayer. However, when graphene is pressed onto silicon

wafer, it could not be detached from silicone. This may be caused by the specific adhesive composition used by the manufacturer, and the work of adhesion between graphene and screen protector is much higher than that between graphene and silicon wafer.

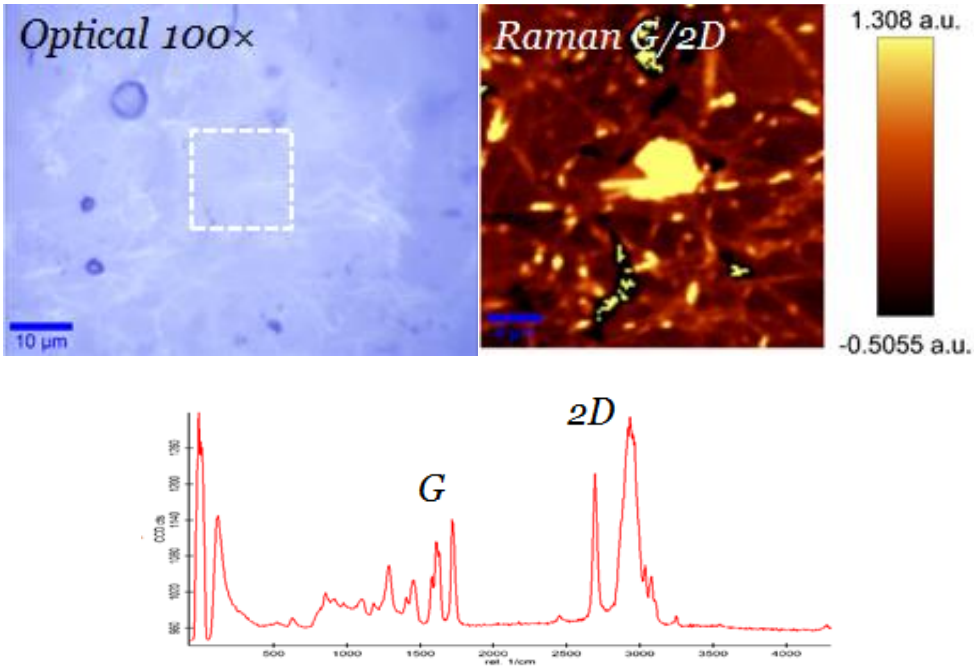

Figure 3.2 Optical image and Raman mapping of graphene on silicone/PET

The failure trial with the commercial screen protector motivated the PDMS-based backing layer design because silicone is basically a slightly modified PDMS. First, a 3mm-thick cured PDMS stamp with 10:1 curing agent ratio is used to transfer CVD graphene, but the result is not satisfactory (Figure 3.3). It is suspected that the bulging of PDMS stamp during graphene adhesion stage tears graphene film apart. Hence, a thinner

PMDS layer is required to reduce this undesirable bulging when PMDS is pressed onto graphene.

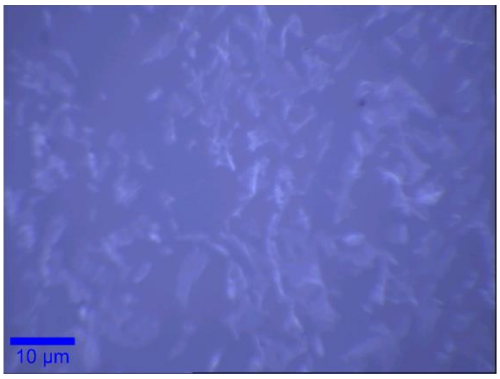

Figure 3.3 Optical image of transferred graphene on PDMS stamp

Since PDMS is soft, the PDMS film will become very flimsy when its thickness is reduced. Therefore, a PET film is used to provide a rigid support for the thin PDMS film. PDMS is spin coated onto PET film with 25 µm thickness and cured in 70℃ for 8 hours (Figure 3.4).

Figure 3.4 Schematic illustration of graphene transfer with cured PDMS on PET

Two curing agent ratios, 10:1 and 50:1 are used in this experiment. The optical images and Raman peaks of the transferred graphene are shown in Figure 3.5. Cracks are generated in both tests, but the flake size of the transfer with 50:1 curing agent ratio is larger. Nevertheless, the graphene on PMDS with 50:1 curing agent ratio cannot be

further transferred onto the silicon wafer. As comparison, graphene on PDMS with 10:1 curing agent ratio can be easily transferred.

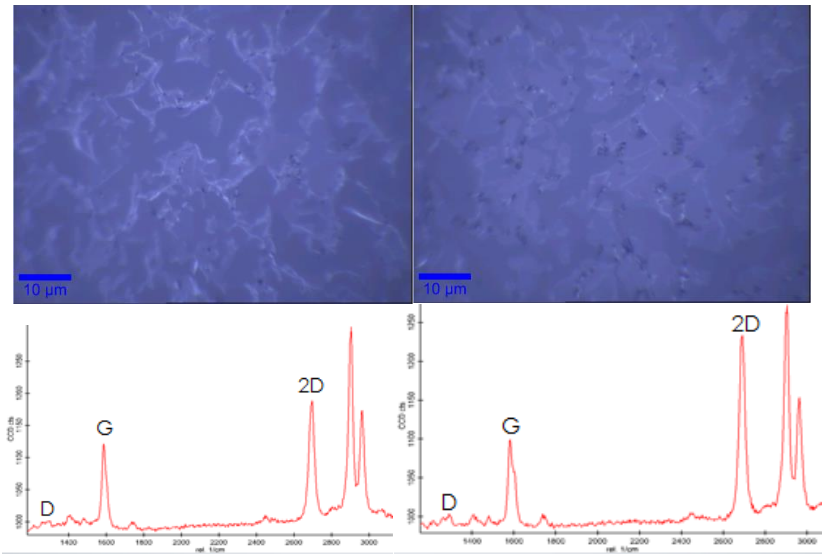

10:1 curing agent ratio 50:1 curing agent ratio

Figure 3.5 Optical image and Raman peaks of transferred graphene on PDMS/PET

Since the graphene surface is stepped as the result of the grain boundaries on copper foil, the smooth surface of cured PDMS could not conform to the surface morphology of graphene. Small gaps will be generated between two surfaces, which later on destroy the graphene film during the delamination process.

To achieve a conformal contact between graphene and PDMS, liquid PDMS precursor is used instead of cured PDMS as the way liquid PMMA is used in graphene transfer. Liquid PDMS with 10:1 curing agent ratio is coated on the graphene/copper sample by both spin coating and dip coating. During the dip coating process, liquid

PDMS is contained in a petri dish, and graphene/copper sample is floated on top of the liquid with graphene contacting PMDS. Then curing process takes place under the same condition used in the previous experiments: 8 hours under 70 ℃. The schematic illustration for both the dip coating test and spin coating test are shown in Figure 3.6. The thickness of the cured PDMS is 3 mm and 25 μm for dip coating and spin coating respectively.

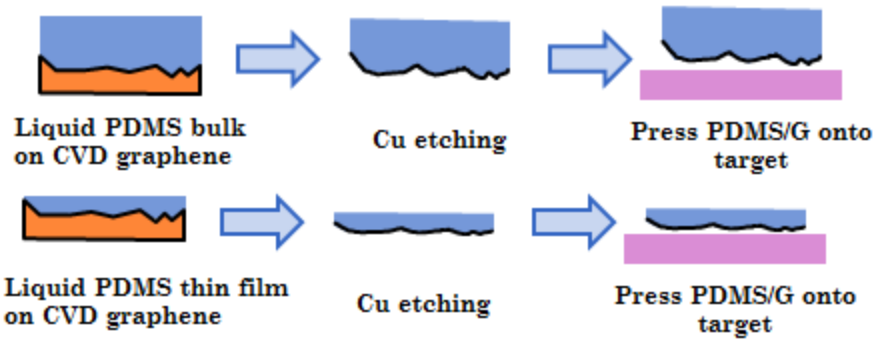

Figure 3.6 Schematic illustration of graphene transfer with liquid PDMS precursor by dip coating (top) and spin coating (bottom)

The transferred graphene has fewer cracks on PMDS, and its monolayer nature is verified by Raman spectroscopy (Figure 3.7). Fluid PDMS precursor could penetrates into the intrinsic wrinkles in the graphene film, so cracking is less likely to happen during the delamination process.

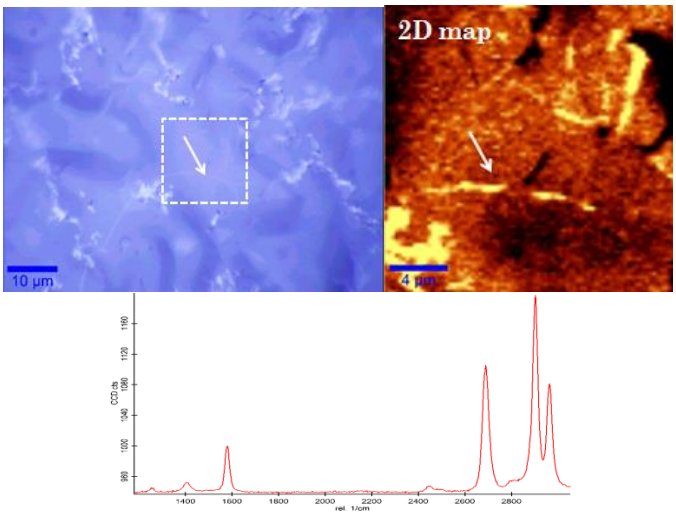

Figure 3.7 Optical image and Raman mapping of transferred graphene in PMDS dipping test

The continuous graphene film on PDMS is further transferred to the target substrate – silicon wafer. The optical image indicates a bad the transfer result (Figure 3.8). Only tiny flakes of graphene are deposited on the surface of the silicon wafer which is not suitable for device fabrication. Again, the bulging effect of the thick PDMS layer during compression induced the shattered graphene on silicon wafer.

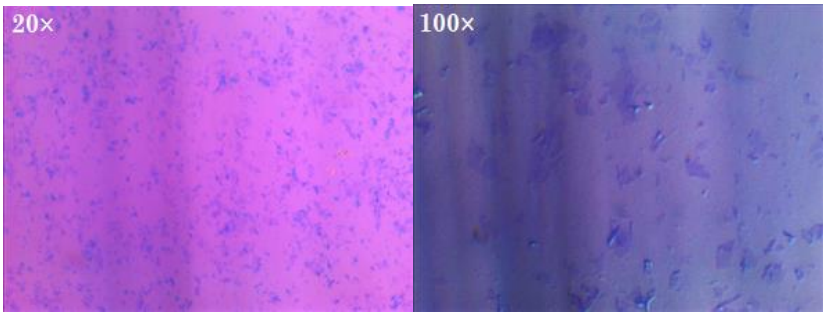

Figure 3.8 Optical image of graphene further transferred on silicon wafer in PDMS dipping test

In the spinning coating test, liquid PDMS with two curing agent ratios are used (10:1 and 30:1), and graphene on both samples can be successfully transferred onto silicon wafer. The optical image and Raman mapping of graphene on PDMS are shown in Figure 3.9. Though cracks are still observed, the flake size of the transferred graphene has reached 20 μm on the PDMS with 30:1 curing agent ratio, so field-effect transistor can be made.

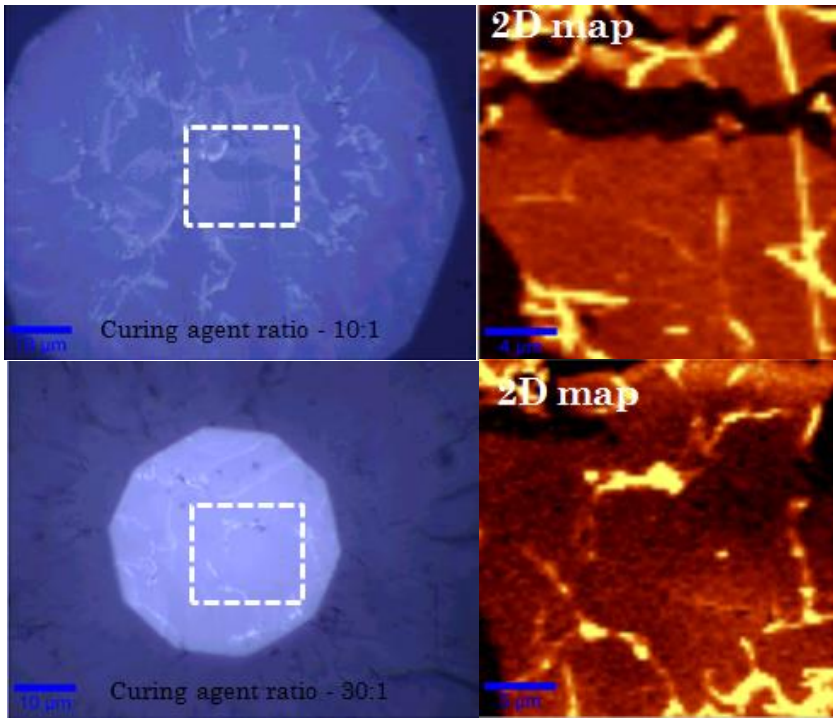

Figure 3.9 Optical images and Raman mappings of transferred graphene on PDMS in spin coating test

Graphene on the spin-coated PDMS film is pressed onto silicon wafer (Figure 3.10). From the microscope image, it can be seen that a ring-shaped graphene layer has

been deposited. The transferred graphene quality in some localized region has improved significantly than the previous results.

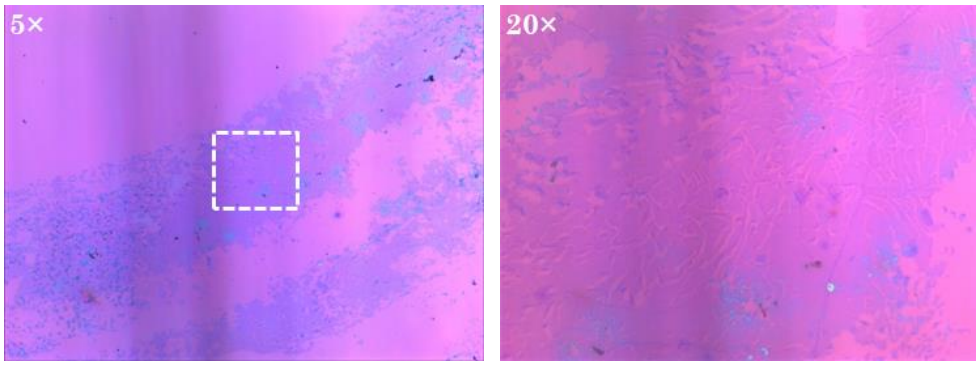

Figure 3.10 Optical image of graphene further transferred on silicon wafer with PDMS spin coating (10:1 curing agent ratio)

The ring-shaped graphene on silicon wafer is suspected to be caused by the curved surface of spin-coated PDMS layer, so the profile of the PDMS layer is analyzed with profilometer. The result shows that an axially symmetric shape with shallow inner region is developed in PDMS during spin coating (Figure 3.11). Therefore, only the graphene on the outter region of the PDMS layer are pressed onto silicon wafer.

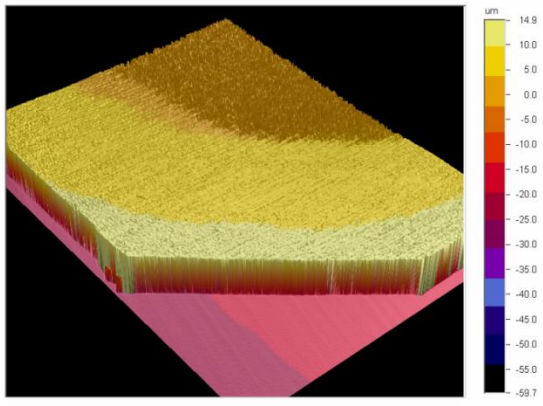

Figure 3.11 Profile of spin-coated PDMS

To achieve a thin flat PDMS layer, a new transfer scheme is developed to incorporate dip coating as well as thin film thickness by pressing liquid PDMS precursor with a flat plate (Figure 3.12). Acrylic plate is used to apply a uniform pressure on PDMS because it can be separated from PDMS after curing. The PMDS curing agent ratio used in this test is 10:1.

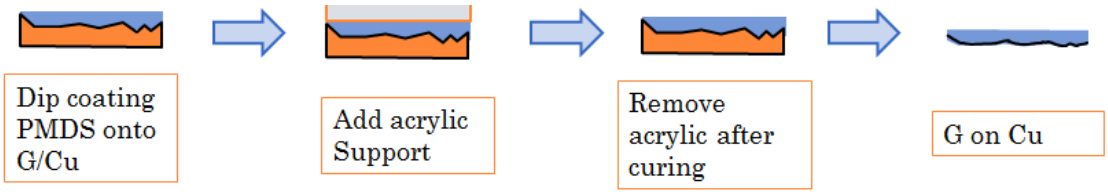

Figure 3.12 Schematic illustration of graphene transfer with PDMS dipping followed by flattening with a smooth acrylic plate

The transferred graphene quality on PDMS is similar to that of the spin coating test (Figure 3.13). The largest graphene flake size achieved is around 30 μm.

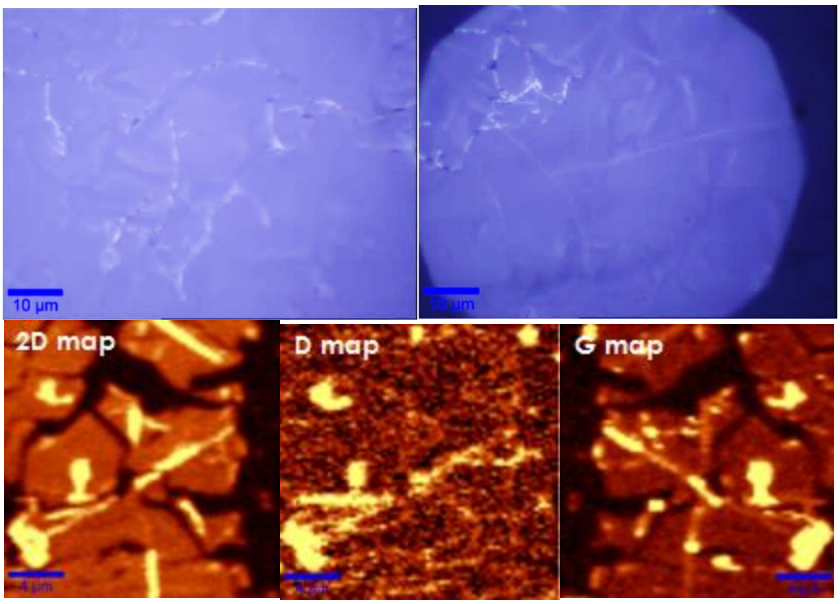

Figure 3.13 Optical image and Raman mapping of graphene on thin PDMS layer made by acrylic plate pressing

However, similar "edge effect" happened again when graphene on PDMS is attached to silicon wafer. Only the graphene on the edge of the square sample are transferred successfully (Figure 3.14). Since spin coating is not used in this experiment, the dome-shaped PDMS is not induced by the centrifugal force generated during spining. Rather, this "edge effect" is due to the deformation of the copper foil after the pressure on acrylic is released. Higher stress in the liquid PDMS is generated during pressing at the center of the graphene/copper sample. When pressure disappears, the residual stress in liquid PDMS will suck the copper foil to bend inward to the center of the graphene/copper film. The dome developed at the graphene center will be preserved after PDMS is cured and copper foil is delaminated. Therefore, the graphene at the center of this dome will not make contact with silicon wafer in the last transfer phase.

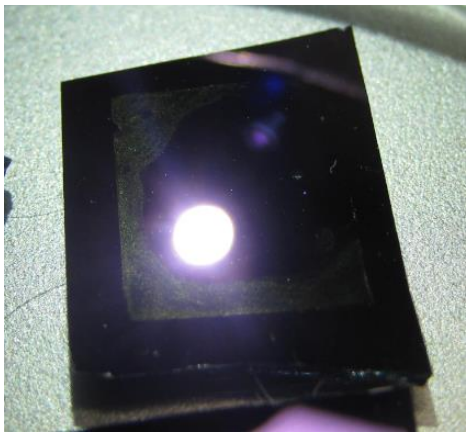

Figure 3.14 “Edge effect” of graphene transferred on silicon wafer

To avoid the “edge effect”, a double-sided transfer scheme is proposed, which is exactly the same as the previous method except that graphene grown on both sides of the copper foil are transferred simultaneously (Figure 3.15). With this symmetric sandwich structure, copper foil will not be bent to either side upon pressure release. In addition, this design also doubles the overall graphene yield.

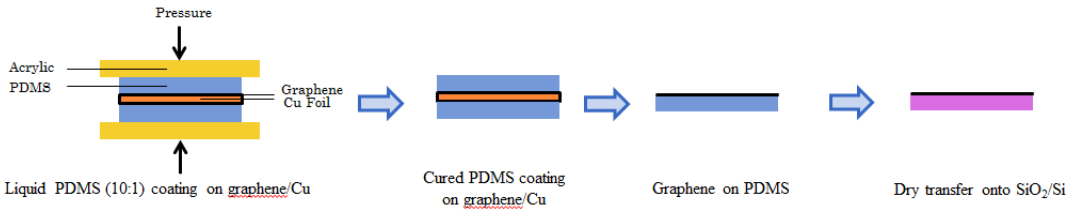

Figure 3.15 Schematic illustrastion of graphene transfer with PDMS dipping and flattening with acrylic plates on both sides

A detailed transfer procedure is described as follows:

Step 1: Liquid PDMS (polymer kit Sylgard 184, Dow Corning) with 10:1 curing agent ratio is degased and coated on both sides of the graphene/Cu foil, and two pieces of flat acrylic plates are pressed on PMDS from top and bottom to achieve a uniform PDMS thickness. When applying acrylic to the liquid PDMS, pressure should be initiated from one edge of the sample and smoothly travels across the entire surface to prevent bubble formation in liquid PDMS.

Step 2: The sample is secured in the environment chamber and liquid PDMS is cured under 70°C for 8 hours. After PDMS is cured, acrylic plates are removed to assist the graphene delamination process.

Step 3: Graphene is delaminated from the copper foil and stays on the cured PDMS layer. Two methods can be used for this step: traditional wet etching and electrochemical delamination. The later one is used in this experiment. An aqueous 0.5M sodium sulfate solution is used as the electrolyte, PDMS/graphene/Cu is used as the cathode, and a platinum mesh is used as an inert anode. A 15V DC power supply is used in the electrolysis process.

Step 4: This step is optional since graphene/PDMS/rigid plastic film can be the final product of the transfer process. In order to demonstrate that the graphene on PDMS is readily transferrable onto another target substrate, the graphene on PDMS film is pressed against a silicon wafer. A second silicon wafer is used to apply uniform pressure on top of the PDMS layer.

Step 5: Witec Alpha 300 micro-Raman confocal microscope is used to characterize the transferred graphene properties on the PDMS layer, and FEI Quanta-600 FEG Environmental SEM is used to detect the graphene coverage on silicon wafer.

Finally, a thin and flexible plastic film is added onto PDMS to provide a rigid support, so that the perturbations encountered during electrochemical delamination can be blocked from graphene. PEN film is used in this test. Acrylic plates are still used to exert a uniform pressure on the plastic/PDMS/graphene/copper structure, and they can be removed before the curing process (Figure 3.16). Most importantly, this polymer support design can be implemented into a roll-to-roll graphene transfer process. Three different thickness (77 µm, 120 µm, and 225 µm) of the plastic film is used to verify the effectiveness of the additional semi-rigid plastic support.

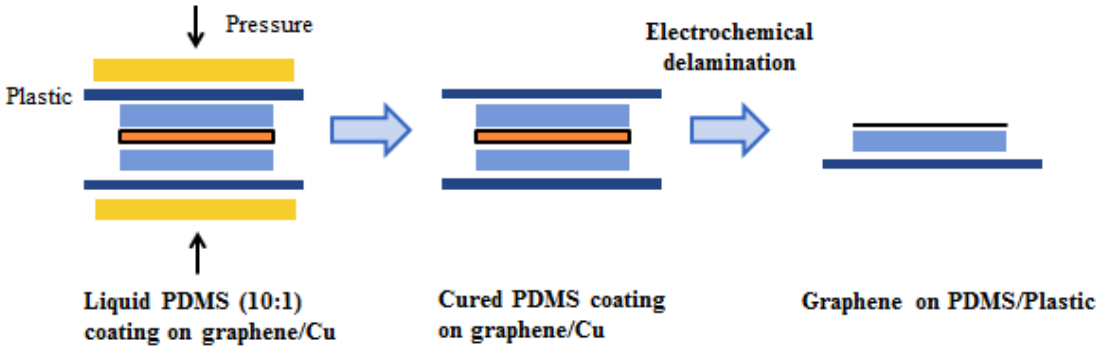

Figure 3.16 Schematic illustrastion of graphene transfer with PDMS dipping and plastic film on both sides

The result of two aforementioned double-sided graphene transfer processes is included in section 3.2.4.

3.2.3 Electrochemical delamination

Like the PMMA-assisted transfer, copper foil can be etched away by ferric nitrate solution or other copper etchant. However, the double-sided graphene transfer support structure proposed in this chapter will required a prolonged etching process since only thin edges of the copper foil are exposed in the etchant solution.

Instead, electrochemical delamination, also known as hydrogen bubbling, can be used. It only takes a few seconds, and the copper foil can be recycled for future CVD graphene growth. During the electrolysis process, reduction will happen at the copper cathode and the following reaction will occur:

$$2H_2O(l) + 2e^- = H_2(g) + 2OH^-(aq)$$

Hydrogen bubbles emerge from the edge of the graphene copper interface, and spread to the remaining area as the electrolytic solution permeate through the opened interfacial space [78] (Figure 3.17).

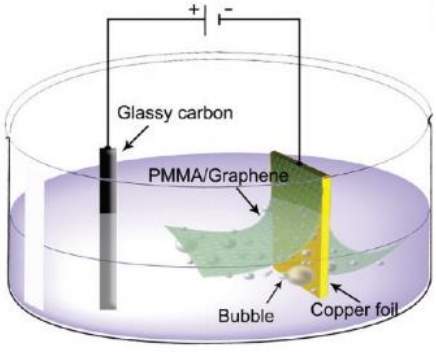

Figure 3.17 Experiment setup for graphene electrochemical delamination [78]

Electrochemical chemical delamination has been used to transfer single-crystal graphene in millimeter size grown on platinum foil via chemical vapor deposition under ambient pressure (Figure 3.18) [79]. The advantage of using hydrogen bubbling over wet etching is that the precious platinum growth substrate can be reused for as many times as desired. Even though a small amount copper will be lost from the surface of copper foil during each hydrogen bubbling process, the copper substrate can also be reused for hundreds of cycles, and the quality of synthesized graphene film will be improved due to the chemical polishing of the copper surface [78].

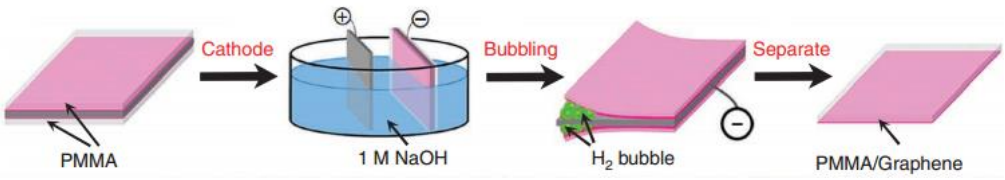

Figure 3.18 Repeated growth and bubbling transfer of graphene on platinum foil [79]

A plastic frame-assisted electrochemical delamination graphene transfer method is also reported (Figure 3.19) [80]. PMMA is used as the intermediate polymer backing layer in this design. After graphene is attached to the target substrate, the plastic film needs to be gently removed by cutting through the entire PMMA layer, and then acetone is used to wash away the remaining exposed PMMA. In comparison, the plastic/PDMS design is more convenient in the final transfer step.

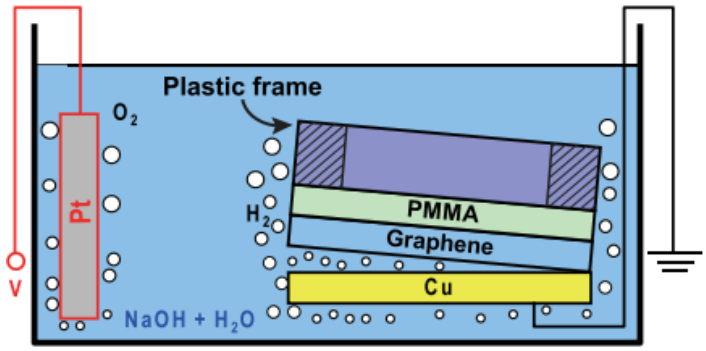

Figure 3.19 Frame-assisted hydrogen bubbling method for graphene transfer [80]

3.2.4 Characterization of transferred graphene film

The transferred graphene on PDMS via double-sided PDMS dipping and pressing with acrylic plates is characterized by optical microscope and Raman spectroscopy (Figure 3.20). Noticeable cracks that are formed in the graphene on PDMS, but the coverage rate is well over 80%, a threshold above which electronic device manufacturing becomes feasible. Two representative dots are selected in the graphene, with the red dot indicating the vacant space and a blue dot indicating the area covered by graphene. As can be seen in the Raman scanning of the blue dot, the high 2D/G ratio proves the graphene film is monolayer, and a low D peak shows that there is no major defect detected locally.

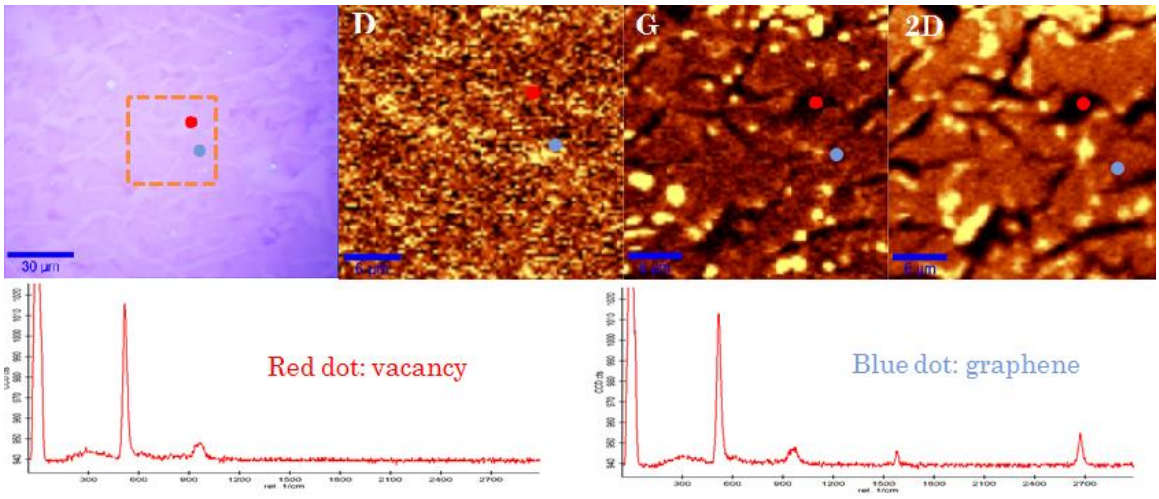

Figure 3.20 Raman spectroscopy of transferred graphene on PDMS with double-sided PMDS dipping and flattening with acrylic plates

Figure 3.21 shows the SEM image of transferred graphene on silicon wafer. As mentioned previously, graphene is pressed on the silicon wafer and the PDMS backing layer is peeled off. The image shows that most part of the graphene film remains intact. The similar graphene coverage rate on both PDMS and silicon wafer indicates a successful transfer as the result of higher work of adhesion between graphene and silicon oxide than that between graphene and PDMS.

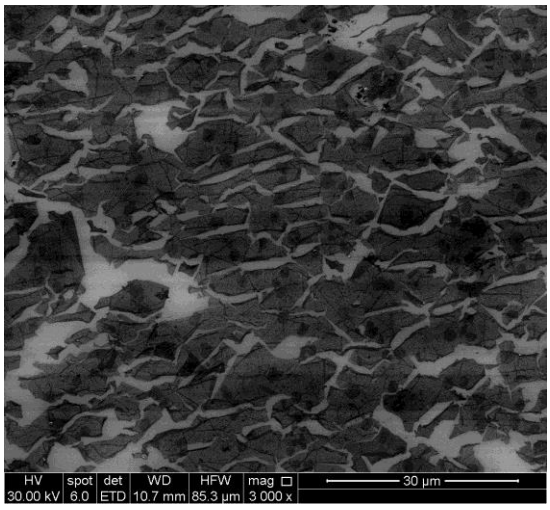

Figure 3.21 SEM image of transferred graphene on silicon wafer with double-sided PMDS dipping and flattening with acrylic plates

The cracks developed in the graphene film are resulted from PDMS swelling and deformation during the electrochemical process. In the follow-up experiment, PEN film is adhered to PDMS to minimize the warping and distortion in PDMS throughout the electrochemical delamination process. Three PEN films with different thickness are used to prove the effectiveness of the plastic frame. From the optical microscope images, a clear trend of larger graphene flake size and fewer cracks can be observed as the thickness of PEN film increases from 77 µm, 120 µm, to 225 µm.

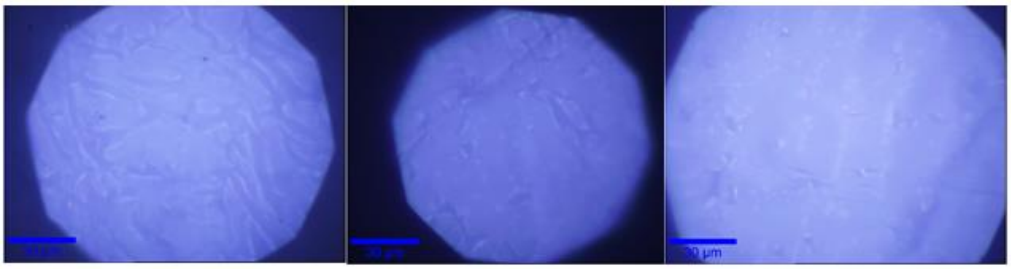

Figure 3.22 Optical images of transferred graphene on PDMS with different plastic frame thickness

3.3 RESULTS AND DISCUSSION

Graphene synthesized via chemical vapor deposition on copper foil is transferred with a commercial screen protector composed of silicone and PET film, a 3-mm cured PDMS stamp, a 25-μm PDMS film on PET, spin-coated liquid PMDS precursor, dip-coated PDMS liquid precursor, dip-coated PDMS liquid precursor followed by flattening with acrylic plates, dip-coated PDMS liquid precursor followed by flattening with acrylic plates from both sides, and finally dip-coated PDMS liquid precursor followed by PEN lamination from both sides.

The quality of graphene transferred with liquid PDMS precursor has fewer cracks and larger flake size because polymer in liquid phase can easily penetrate into intrinsic wrinkles in the CVD graphene film. Smaller PDMS thickness is better in further transferring graphene onto silicon wafer as the bulging effect during adhesion is minimal. To achieve a flat PDMS layer, a double-sided design is proposed to achieve a symmetric loading on both sides of the graphene/copper film and warping in the PDMS is prevented thusly. At last, a semi-rigid flexible plastic layer, e.g. PEN or PET, can provide rigid support to the soft PDMS layer so that less perturbations are acted on graphene during the rest of the transfer process.

3.4 CONCLUSIONS

CVD graphene on copper foil is transferred with liquid PDMS to make conformal contact, and a flexible plastic substrate is adhered to PDMS from both sides to offer a rigid support. Electrochemical delamination is used to separate graphene from copper

foil. The graphene/PDMS/plastic film itself is a good candidate for flexible electronics fabrication since the residue-free graphene coverage is well over 80% and the soft PDMS elastomer can provide effective strain isolation to protect the devices made out of transferred graphene film. In addition, the graphene on PDMS can be further transferred onto silicon wafer or other rigid or flexible substrates. Finally, a roll-to-roll graphene transfer machine can be designed with this double-sided bilayer polymer support transfer scheme, which is presented in Chapter 5.

Chapter 4 Strain Isolation Effect of PDMS

4.1 INTRODUCTION

Graphene-based electronics can maintain its functionality under large deformation, and it has a wide range of application including touch screens, OLEDs, LCDs, solar cells, and wearable electronics. Devices made with graphene need to be protected from external loads encountered in normal use of the product. The design of combining a soft PDMS layer and a semi-rigid plastic layer as described in Chapter 3 has the strain isolation effect that can allow large distortion of this multi-layer structure without permanently damaging the patterned graphene devices on PDMS. The strong mechanical strength of the bottom plastic film also makes the entire structure suitable for a roll-to-roll transfer process.

The soft PDMS layer is effective in reducing the transmission of strain developed in the plastic substrate at the bottom to the electronics layer at the top. Similar strain isolation design is used to protect inorganic electronic devices [81]. A shear-lag model can be used to describe the strain variation from the device to the flexible substrate, and it has been found that the strain isolation effect becomes better as the PDMS layer thickness increases and the patterned device size decreases [68, 82-84]. In the Si/PDMS/plastic structure reported by Kim, Dae-Hyeong, et al., the strain developed in the top Si layer is more than 200 times lower than the strain in the stretched plastic layer at the bottom [69]. The characteristic length, Λ, measures the distance over which normal strain builds up in the islands [82]. Hence, greater Young's modulus of the device, thicker device and PDMS layer, as well as higher PDMS shear modulus can lead to better strain isolation design.

$$\Lambda = \sqrt{\frac{E_{Device} Hh}{\mu_{PDMS}}}$$

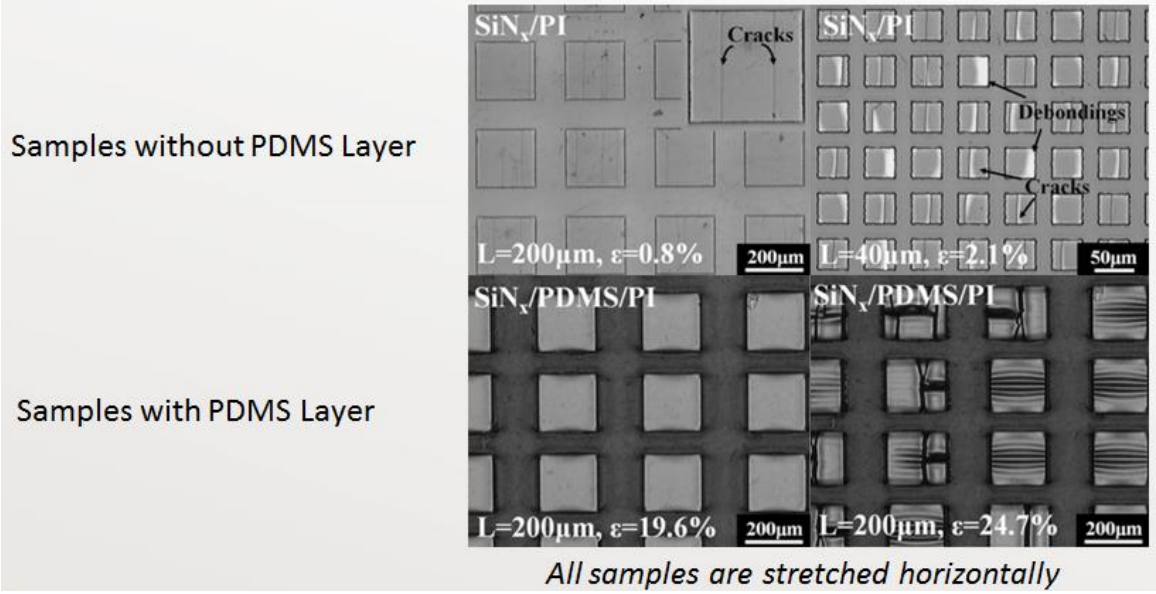

Figure 4.1 PDMS strain isolation effect for SiN islands on polyimide [82]

4.2 MODELING OF STRAIN ISOLATION EFFECT

The use of PDMS in the bilayer graphene transfer design could also help to shield the externally applied strain in the plastic substrates from the delicate graphene devices. Even though, the strain isolation effect of PDSM is proven for inorganic devices, its effectiveness remains to be verified for graphene-based electronics due to the one-atom thickness nature of this 2D material. The equation below shows a comparison between the macroscopic strength of silicon and graphene. It can be seen that though graphene has a higher Young's modulus, its extremely small thickness weakens the overall strength significantly.

$$\frac{E_{Graphene}h_{Graphene}}{E_{Si}h_{Si}} = \frac{1TPa * 0.34nm}{130GPa * 0.3\mu m} = 0.0087$$

Both analytical model and finite element analysis are used to measure the strain isolation effect of adding an intermediate PDMS layer between graphene islands and plastic substrate.

4.2.1 Analytical model

The analytical model employs the existing analysis for inorganic devices on plastic substrates, and four major assumptions are made to make the model valid, and the schematic illustration of this analysis is shown in Figure 4.2 [68].

1. Graphene is perfectly bonded with either PDMS or the plastic substrate.

2. Graphene is much thinner than both PDMS layer and plastic substrate.

3. The PDMS layer can be modeled as a shear lag to transmit non-uniform shear stress between the device and substrate.

4. The bending rigidity of the graphene device is negligible.

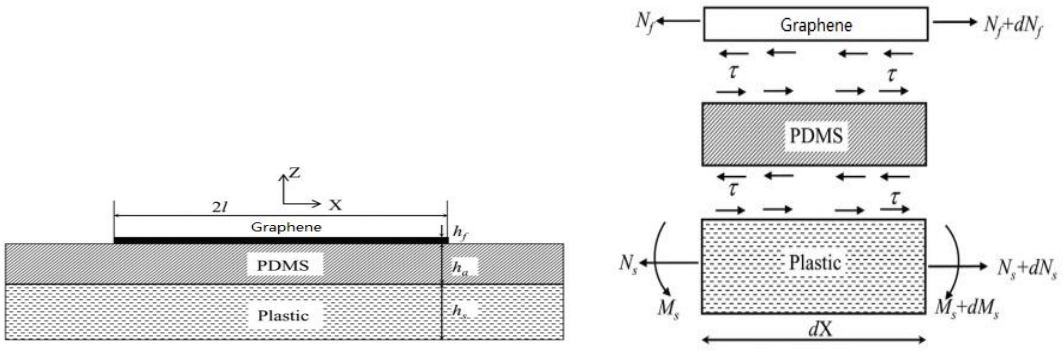

Figure 4.2 Analytical model of the strain isolation effect of PDMS [68]

The constitutive relations and equilibriums of force and moment are established for each of the three layers as follows [68].

1. Graphene device layer

Force equilibrium: $\frac{dN_f}{dX} - \tau = 0$ (1)

N_f: axial force in the device per unit width.

τ: shear stress.

Also, $N_f = \frac{\overline{E_f} h_f du_f}{dX}$ (2)

h_f: graphene thickness

The plain strain modulus: $\overline{E_f} = \frac{E_f}{1-{\upsilon_f}^2}$ (3)

υ_f: Poisson's ratio of graphene

Traction-free boundary conditions at the edges of the graphene film:

$N_f = 0$ at X=$\pm l$

2. Strain isolation layer

Shear stress: $\tau = G_a(\frac{\partial u_a}{\partial Z} + \frac{dw}{dX})$ (5)

Based on shear lag model: $\frac{\partial u_a}{\partial Z} \approx \frac{\Delta u}{h_a}$ (6)

h_a: thickness of the strain isolation layer

u_a: axial displacement

G_a: shear modulus of the strain isolation layer

Δu is the difference between the axial displacement at two interfaces

Axial displacement at the device-PDMS interface: u_f

Axial displacement at the PDMS-plastic interface: $u_s - \frac{h_s}{2}\frac{dw}{dX}$

Hence, $\tau = [u_f - u_s + \left(h_a + \frac{h_s}{2}\right)\frac{dw}{dX}]\frac{G_a}{h_a}$ (7)

3. *Plastic substrate*

Force equilibrium: $\frac{dN_s}{dX} - \tau = 0$ (8)

Moment equilibrium: $\frac{dM}{dX} + \frac{\tau h_s}{2} = 0$ (9)

Applied force: $N_s = \frac{\overline{E_s} h_s du_s}{dX}$ (10)

Applied moment: M$= -\frac{\overline{E_s} {h_s}^3}{12}\frac{d^2w}{dX^2}$ (11)

Plane strain modulus: $\overline{E_s} = \frac{E_s}{1-\upsilon_s{}^2}$ (12)

h_s: thickness of the plastic substrate

υ_s: Poisson's ratio of the plastic substrate

Boundary conditions:

N_0 *and* M_0 are applied at the two ends of the substrate

Based on the force and moment analysis for the three layers, the following relation can be derived:

$\frac{d^2\tau}{dX^2} - \lambda^2\tau = 0$ (13)

$\lambda = \sqrt{\frac{G_a}{h_a}(\frac{1}{\overline{E_f} h_f} + \frac{4}{\overline{E_s} h_s} + \frac{6h_a}{\overline{E_s} {h_s}^2})}$ (14)

Applying boundary conditions:

$\left.\frac{d\tau}{dX}\right|_{X=\pm l} = -\frac{G_a}{\overline{E_s} h_s h_a}[N_0 + \frac{6M_0(h_s+2h_a)}{{h_s}^2}]$ (15)

Shear stress can be obtained by integration.

$$\tau = -\tau_{max}\frac{\sinh(\lambda X)}{\sinh(\lambda l)} \quad (16)$$

$$\tau_{max} = \frac{G_a}{\lambda \overline{E_s} h_s h_a}\left[N_0 + \frac{6M_0(h_s+2h_a)}{{h_s}^2}\right]\tanh(\lambda l) \quad (17)$$

The maximum strain in the device is located at the center.

$$\epsilon_{f,max} = \frac{\tau_{max}}{\lambda \overline{E_f} h_f}\tanh(\frac{\lambda l}{2}) \quad (18)$$

Strain isolation is defined as the ratio between the maximum strain developed in the device with the PDMS layer and the maximum strain developed in the device without the PDMS layer.

For pure tension, the maximum strain developed in the device without the PDMS layer can be calculated based on beam theory:

$$\varepsilon_{f,max}{}' = \frac{N_0}{\overline{E_f} h_f + \overline{E_s} h_s} \quad (19)$$

$$Strain\ Isolation = \frac{\varepsilon_{f,max}}{\varepsilon_{f,max}{}'} \approx (\frac{1}{\overline{E_f} h_f} + \frac{1}{\overline{E_s} h_s})\frac{G_a(2l)^2}{8h_a} \quad (20)$$

The approximation is made assuming that the device size is much smaller than the substrate size, e.g. $\lambda l \ll 1$

For pure bending, the maximum strain developed in the device without the PDMS layer can also be calculated based on beam theory:

$$\varepsilon_{f,max}{}' = \frac{6M_0}{h_s(4\overline{E_f} h_f + \overline{E_s} h_s)} \quad (21)$$

$$Strain\ Isolation = \frac{\varepsilon_{f,max}}{\varepsilon_{f,max}{}'} \approx (\frac{1}{\overline{E_f} h_f} + \frac{4}{\overline{E_s} h_s})(\frac{1}{h_a} + \frac{2}{h_s})\frac{G_a(2l)^2}{8} \quad (22)$$

Again, the device size is assumed to be much smaller than the substrate size, e.g. $\lambda l \ll 1$.

The following design parameters are used to calculate the strain isolation for pure tension and pure bending, and same values are used in the simulation for comparison.

$$h_f = 400 \text{ nm } h_a = 25 \text{ µm } h_s = 25 \text{ µm } 2l = 40 \text{ µm}$$

$$E_f = 1 \text{ TPa } G_a = 0.676 \text{ MPa } E_s = 2 \text{ GPa } \nu_f = 0.17 \ \nu_s = 0.34$$

For pure tension:

$$\text{Strain Isolation} = \left(\frac{1}{\overline{E_f} h_f} + \frac{1}{\overline{E_s} h_s}\right)\frac{G_a (2l)^2}{8 h_a} = 0.000109$$

For pure bending:

$$\text{Strain Isolation} = \left(\frac{1}{\overline{E_f} h_f} + \frac{4}{\overline{E_s} h_s}\right)\left(\frac{1}{h_a} + \frac{2}{h_s}\right)\frac{G_a (2l)^2}{8} = 0.00119$$

Note that the thickness of the graphene layer is assumed to be 400 nm instead of the actual value of single-layer graphene, 0.34 nm, for comparison with the result from simulation. The minimum allowable geometry in the simulation is 400 nm. The properties of the plastic substrate are based on polyimide film.

4.2.2 Finite element analysis

Finite element analysis is used to simulate the strain isolation effect of the PDMS layer in pure stretching and pure bending. Kapton, a commercial polyimide film, is used as the base substrate (Figure 4.3).

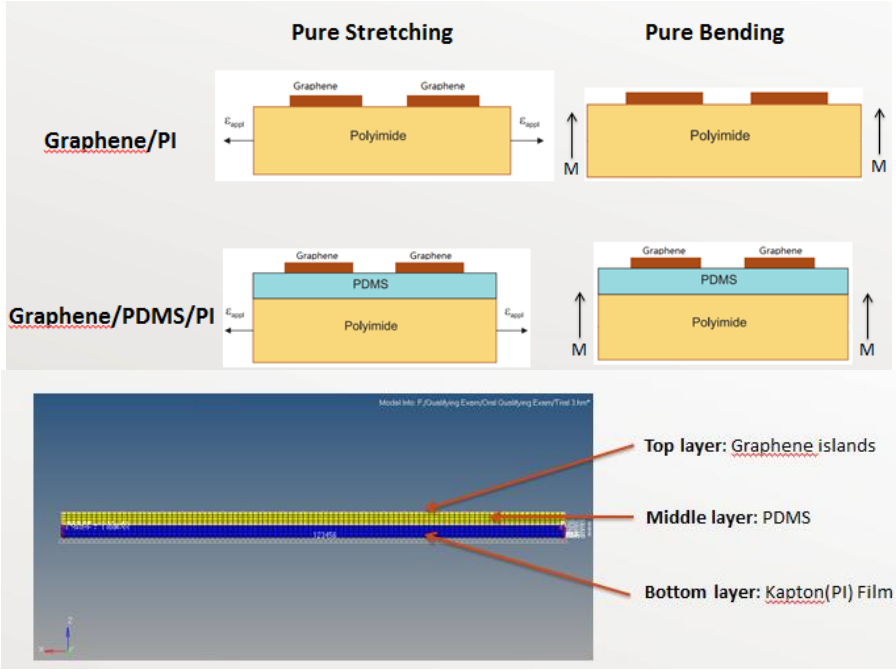

Figure 4.3 Schematic illustration of the models used in simulation

The Young's moduli and Poisson's ratios used in the simulation for graphene, PDMS, and Kapton are listed in Table 4.1.

	Graphene	PDMS	Kapton
Young's modulus	1 TPa	1 MPa	2 GPa
Poisson's ratio	0.17	0.48	0.34

Table 4.1 Young's moduli and Poisson's ratios of the materials used in the simulation

Graphene-based devices are represented by square islands equally spaced on the PDMS or Kapton (Figure 4.4). Same force and moment are applied on the Kapton structure in the models with and without the PDMS layer. The detailed geometry and loads applied in the simulation are listed in Table 4.2. During the simulation, graphene islands are assumed to stay bonded to PDMS or the plastic substrate.

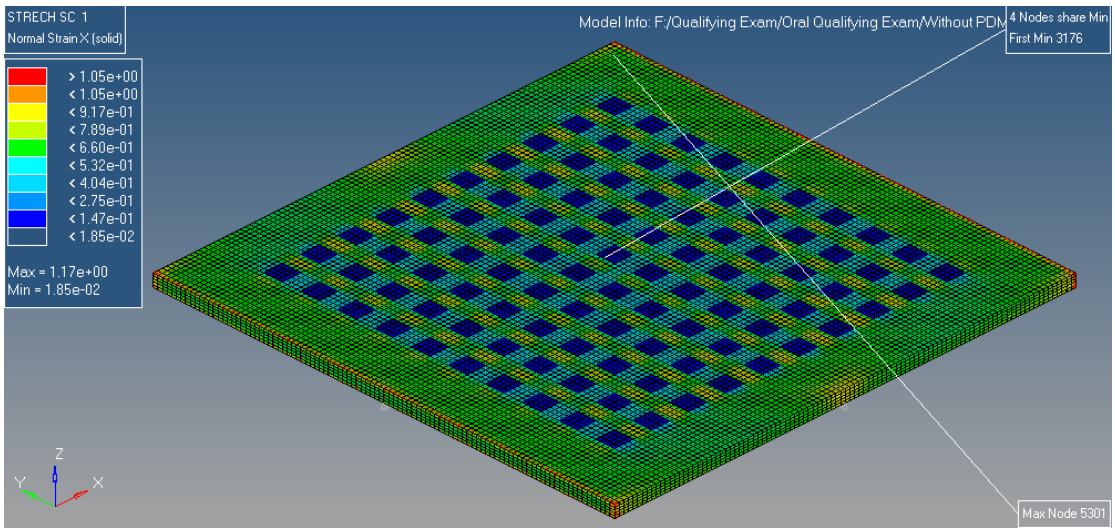

Figure 4.4 Graphene islands are equally spaced on the flexible substrate

Geometry	**Loads**
Substrate size: 1 mm x 1 mm	Force = 50 mN (x-direction)
Graphene island size: 40 μm x 40 μm	
Graphene island spacing: 40 μm	Moment = 0.1 N*mm (y-direction)
Kapton thickness: 25 μm	

Table 4.2 Geometry and loads applied in the simulation

Three boundaries conditions are used in the simulation (Figure 4.5):

1. Only the nodes in the middle of the bottom surface of the PET film are fixed (*y-axis, All 6 DOFs*).
2. In addition to the constraints used in the first case, the nodes in the middle of the bottom surface along x-axis are also fixed. (*x-axis, y-axis, All 6 DOFs*)

3. In addition to the constraints used in the first case, all other nodes at the PET bottom surface are also fixed. (*Constrained DOFs: 3,4,5,6*)

However, the simulation result with the first boundary condition does not converge, because the applied load will cause rotation of the film around the constrained nodes. With more constrained nodes, the second and third boundary conditions lead to convergent solutions.

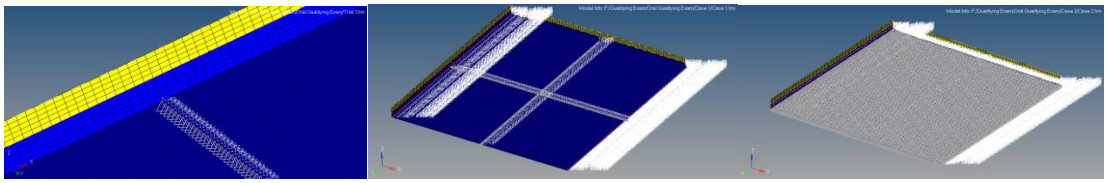

Figure 4.5 Schematic illustration of three boundary conditions used in the simulation

Figure 4.6 shows the simulation result of the same model with boundary conditions 2 and 3. Same node is selected in both cases for comparison, and their corresponding strains are equal. Even though the boundary conditions give the same strain in the graphene devices, the strains developed in the PDMS layer are different with two boundary conditions.

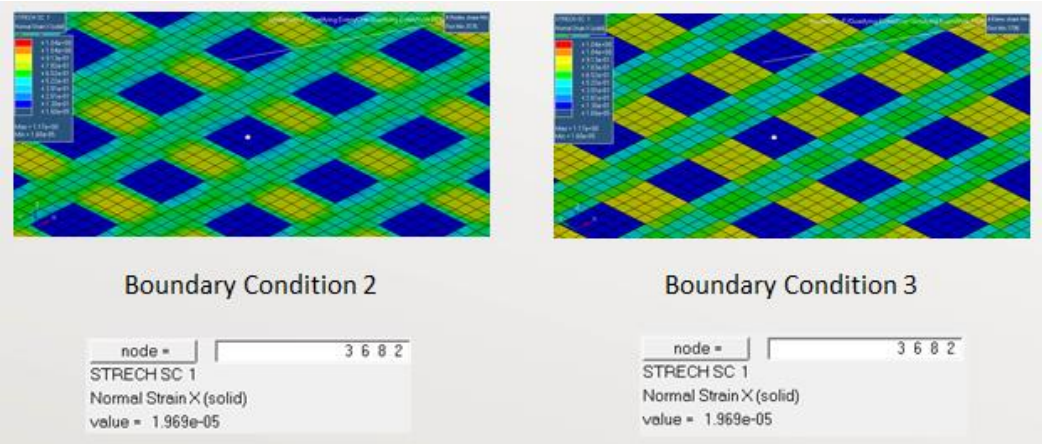

Figure 4.6 Comparison of the simulation results with boundary conditions 2 and 3

The strain isolation effect of the PDMS layer is studied with both boundary condition 2 and boundary condition 3 when pure tension is applied on the flexible substrate. Same nodes in two simulation models are selected for comparison. The strain isolation calculated based on the simulation results are 0.000813 for boundary condition 2 and 0.000696 for boundary condition 3 (Figure 4.7 and Figure 4.8).

Boundary condition 2:

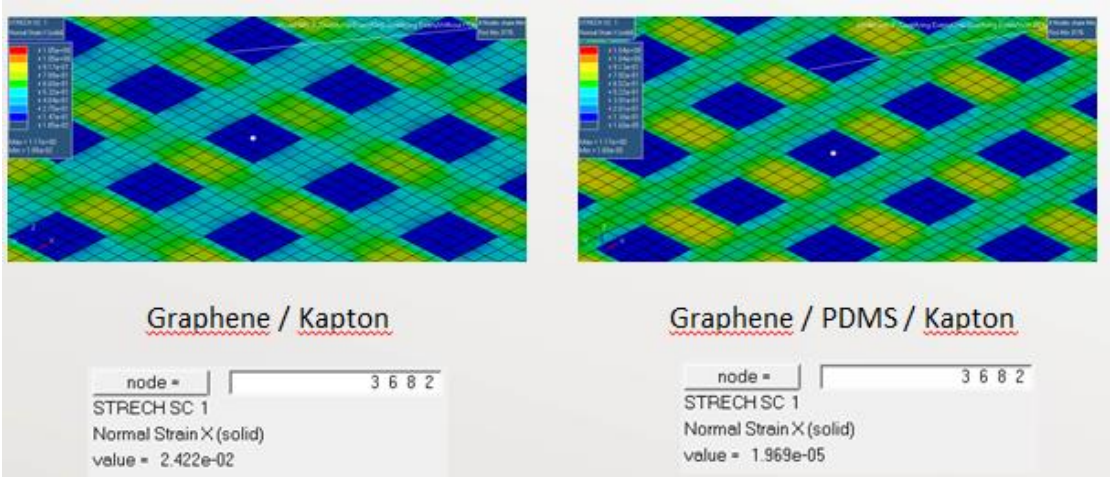

Figure 4.7 Simulated PDMS strain isolation effect (*boundary condition 2*)

$$Strain\ Isolation = \frac{1.969\times10^{-5}}{2.422\times10^{-2}} = 0.000813$$

Boundary condition 3:

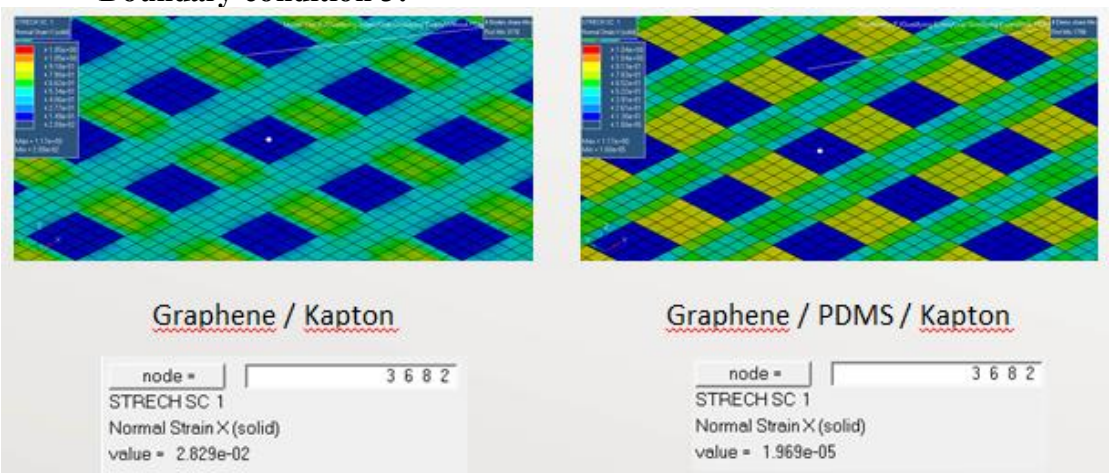

Figure 4.8 Simulated PDMS strain isolation effect (*boundary condition 3*)

$$Strain\ Isolation = \frac{1.969\times10^{-5}}{2.829\times10^{-2}} = 0.000696$$

Next, the strain isolation effect of PDMS is simulated when the flexible substrate is subjected to pure bending. The nodes in the middle plane of the model are fixed to simulate a symmetric deformation (*y-axis, All 6 DOFs*) (Figure 4.9).

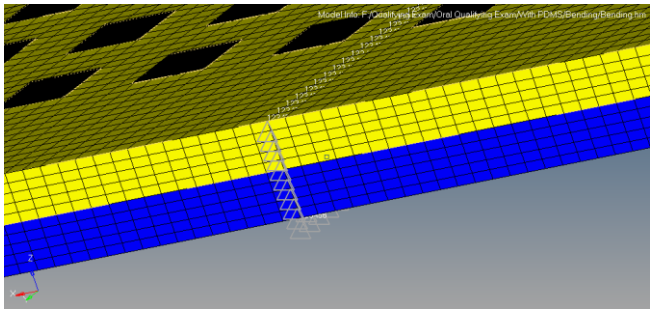

Figure 4.9 Boundary condition used for pure bending

Again, same nodes are chosen in both models for comparison between the strain in the device with and without the elastomeric strain isolation layer. The simulated strain isolation with pure bending is 0.000312 (Figure 4.10).

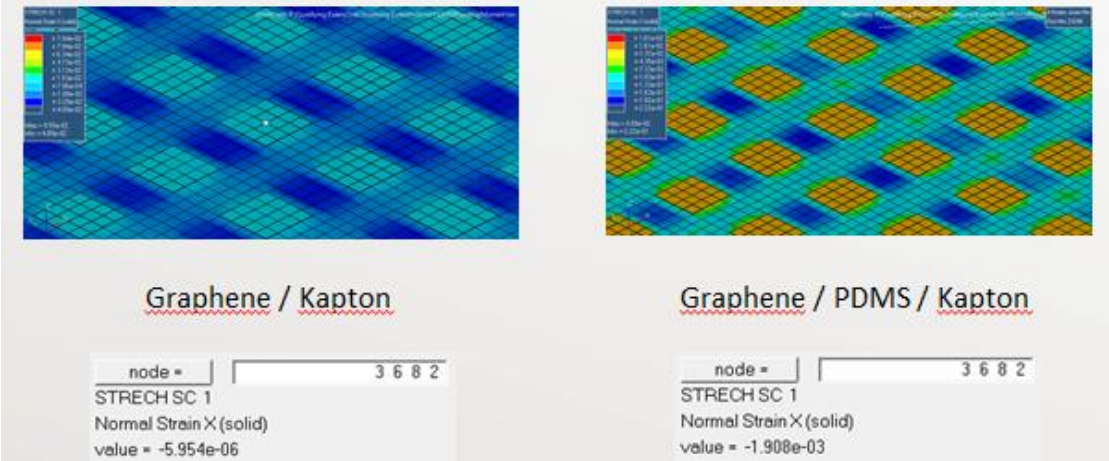

Figure 4.10 Simulated PDMS strain isolation effect for pure bending

$$Strain\ Isolation = \frac{-5.954\times10^{-6}}{-1.908\times10^{-3}} = 0.000312$$

4.3 RESULTS AND DISCUSSION

The strain isolation effect of PDMS is predicted based on the analytical model and the finite element simulation. Under pure tension, the strain isolation is calculated to be 0.000109 from the analytical model. The simulated strain isolation for pure tension is 0.000813 or 0.000696 depending on the different boundary conditions used. The results from both methods for pure tension are on the same order of magnitude. Under pure bending, the analytical strain isolation is 0.00119 and the simulated strain isolation is 0.000312, which are also comparable in magnitude. Since small difference in boundary

conditions could lead to relatively large change in the simulation result, the strain isolation predicted from both the analytical mode and finite element simulation is valid.

In addition, the relation between the strain isolation effect and the Young's modulus of PDMS as well as its thickness are also studied. Depending on the concentration of the curing agent used, the Young's modulus of PDMS can vary between 0.2 MPa to 2.7 MPa (Figure 4.11) [85]. In the simulation, two Young's moduli of PDMS within this range are applied, which are 0.5 MPa and 1MPa.

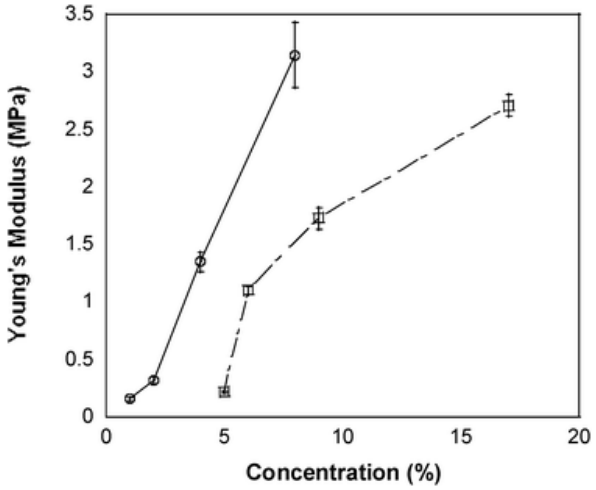

Figure 4.11 Young's modulus of PDMS with different curing agent ratios

The ratio of the strains developed in graphene device with 1 MPa PDMS and 0.5 MPa PDMS is 1.998. From this simulation result, it can be concluded that smaller PDMS Young's modulus will result in better strain isolation effect (Figure 4.12). Same conclusion can be drawn from the analytical model since Young's modulus of PDMS is in the denominator of the expression for strain isolation.

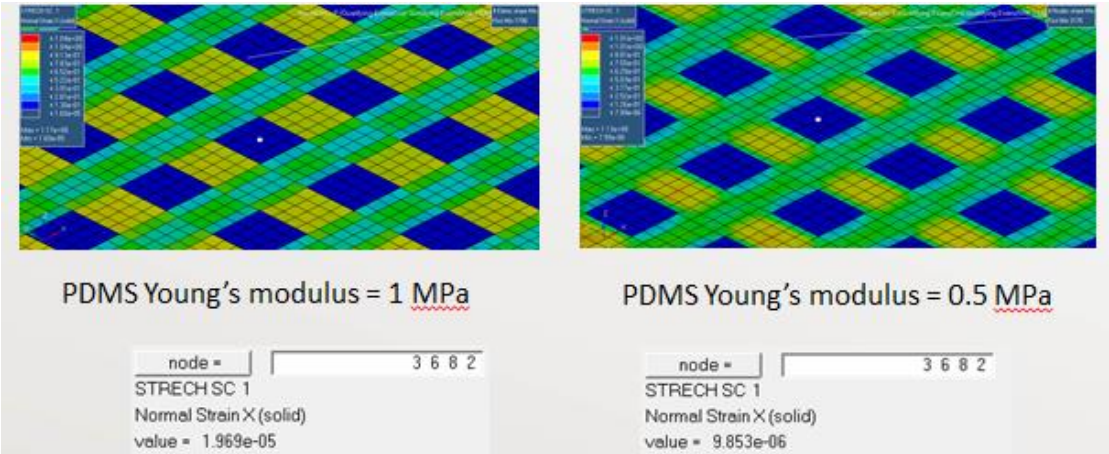

Figure 4.12 Effect of Young's modulus of PDMS on strain isolation

$$\text{Strain Ratio} = \frac{1.969\times10^{-5}}{9.853\times10^{-6}} = 1.998$$

Furthermore, different thickness of the PDMS layer is used to test its effect on strain isolation. The strain developed in the graphene device with 10 μm PMDS layer is 1.18 times higher than the strain developed in the model with 25 μm PMDS layer, so thicker PDMS layer will lead to better strain isolation effect (Figure 4.13). This conclusion is also consistent with the analytical model.

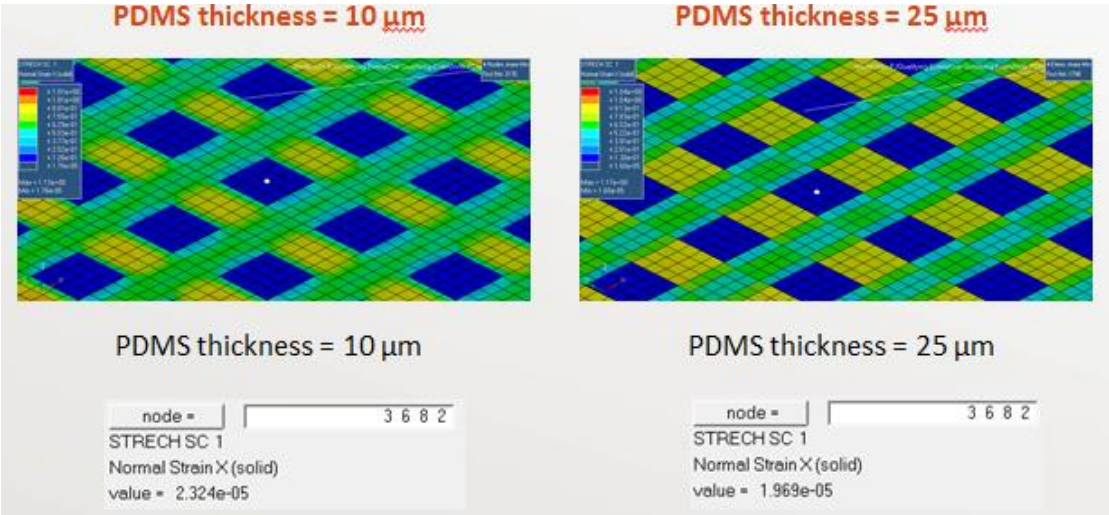

Figure 4.13 Effect of PDMS layer thickness on strain isolation

$$\text{Strain Ratio} = \frac{2.324\times10^{-5}}{1.969\times10^{-5}} = 1.18$$

4.4 CONCLUSIONS

Graphene-based devices are regarded as a potential candidate for post-silicon electronics, especially in the field of flexible electronics. Due to the one-atom thickness and stepped surface generated during chemical vapor deposition, electronics made with graphene are prone to cracks, so proper protection mechanism is necessary to block external loads.

By adding an intermediate PDMS layer, the strain transmission from the plastic substrate to graphene devices can be effectively reduced. The strain isolation effect of PDMS is verified with both analytical model and simulation. Furthermore, it is found that thicker PDMS layer and lower Young's modulus of PDMS will lead to better strain isolation effect.

Chapter 5 Roll-to-roll Graphene Transfer Machine Design

5.1 Review on current roll-to-roll graphene transfer design

Roll-to-roll equipment is extensively used in industrial fabrication of electronic products. To realize the production of graphene-based electronics in a large scale, an efficient roll-to-roll graphene transfer machine is necessary. This concept has already been attempted by several companies in the electronics industry. For example, Sony reported their lasted progress on roll-to-roll graphene production and transfer machine in early 2013 (Figure 5.1).

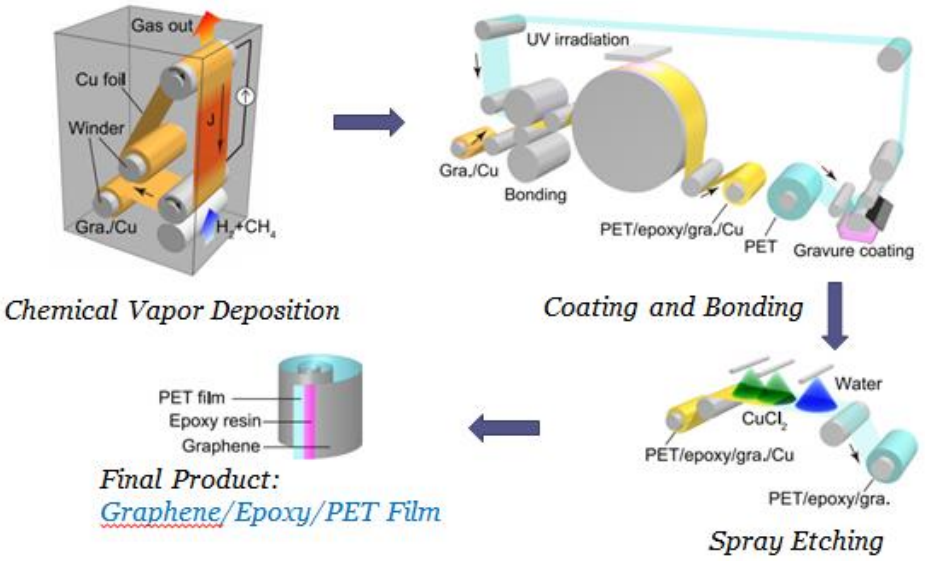

Figure 5.1 Roll-to-roll production of 100m graphene film by Sony Corp. [86]

Epoxy is used in this design to create a strong bond with graphene and PET film. The epoxy is photocurable by UV light, so polymer curing is avoided. Wet etching is

used to remove the copper growth substrate, and the final product of this roll-to-roll process is a three-layer conductive film made with graphene, epoxy, and PET. However, there are a few disadvantages associated with this design.

First, epoxy is a permanent adhesive, so graphene transferred onto epoxy could not be further delaminated. Second, graphene grows on both sides of the copper foil, but only one side is transferred in this design. Moreover, copper foil is not recycled in this process which raises the cost per unit production.

Based on the double-layer polymer support design discussed in Chapter 3, the roll-to-roll transfer machine should be designed to transfer graphene on both sides of the copper foil simultaneously. A classical double-sided laminating machine is used as a reference (Figure 5.2) [87].

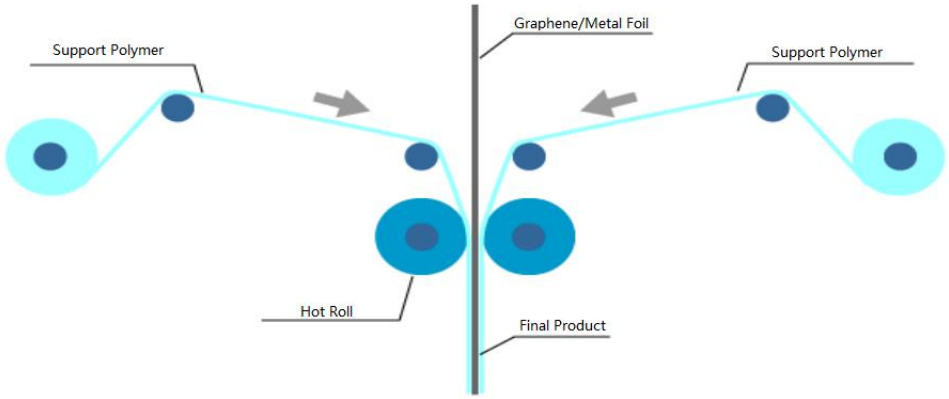

Figure 5.2 Double-sided polymer lamination [87]

Several concepts are generated to implement this double-sided design, and electrochemical delamination is applied instead of wet etching so that copper foil can be reused and the long etching time encountered in double-sided graphene delamination could be avoided.

5.2 CONCEPT GENERATION AND CAD MODELING

Two preliminary concepts are generated as shown in Figure 5.3 and Figure 5.4, and PDMS curing process is not included. The first concept is a single-sided transfer design, liquid PDMS is dispensed between the plastic film and graphene on copper foil. Two rollers are used to apply a uniform pressure on two films to form a thin PDMS layer.

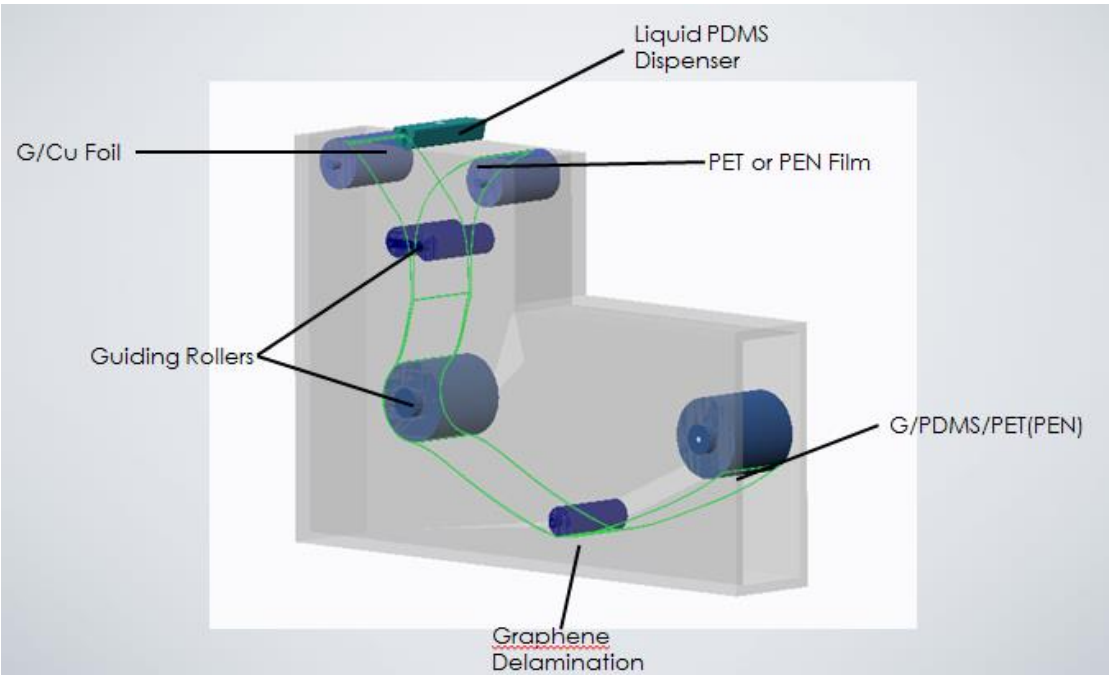

Figure 5.3 Preliminary concept for roll-to-roll graphene transfer #1

The second concept is a double-sided roll-to-roll graphene transfer with a guiding slot design. Since the copper foil used for graphene synthesis is very thin, two shallow slots can be used to align the film with the rollers throughout the transfer process. In addition, the guiding slot can also be used as an electrode during the graphene delamination.

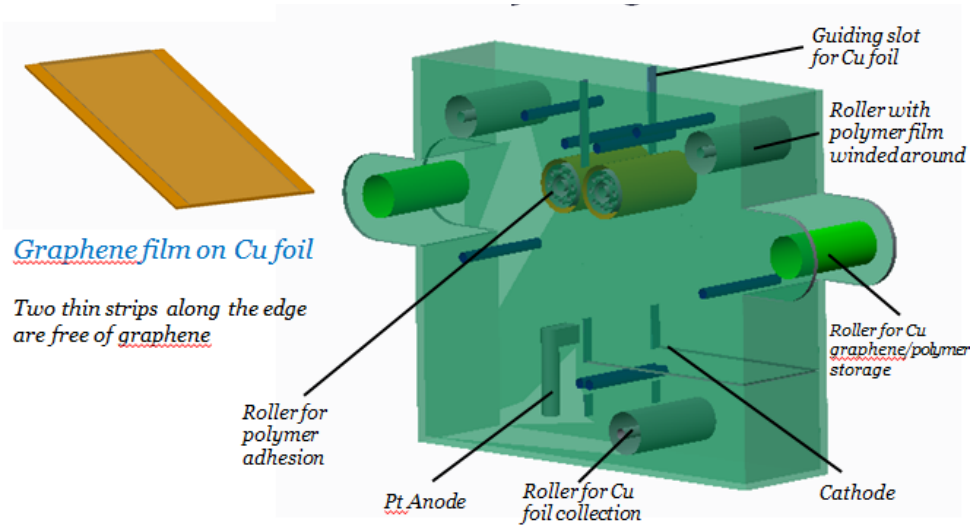

Figure 5.4 Preliminary concept for roll-to-roll graphene transfer #2

One major issue in graphene transfer with liquid PDMS is its excruciatingly long curing time. The requirement for complete PDMS curing is 8 hours under 80°C. Though raising the curing temperature could reduce curing time, but there is not much room for temperature increase since PDMS will lose its integrity around 120°C. To solve this problem, a faster way of PDMS curing is researched.

It is reported that the chemical composition of PDMS can be altered to make it photosensitive by adding photoinitiator into the traditional PDMS liquid precursor [88-

90]. Even though pre-baking and post-baking are required, the overall curing time is significantly reduced. A three-piece roll-to-roll graphene transfer machine is modeled to incorporate the photocurable PDMS with UV radiation (Figure 5.5). Three detachable units are designed to facilitate disassembly and maintenance, which are #1 backing layer adhesion unit (Figure 5.5), #2 electrolysis unit (Figure 5.6), and #3 collection unit (Figure 5.7). The aforementioned polymer adhesion mechanism and guiding slot design are implemented in this model.

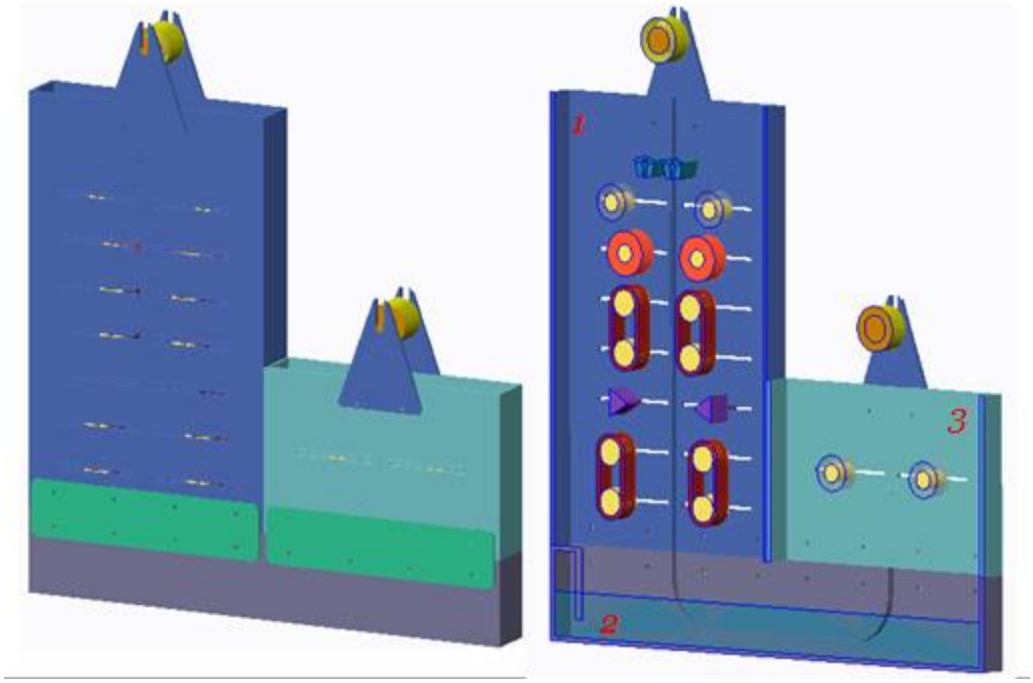

Figure 5.5 Three-unit detachable machine for roll-to-roll graphene transfer

The backing layer adhesion unit consists of a PDMS dispenser, double compressive rollers for lamination, a soft baking belt, a UV radiation source, and a hard baking belt (Figure 5.6). All the functional components in this unit can be moved horizontally with adjustable the fasteners in the corresponding slots. Furthermore, two

sliding blocks attached to both ends of a spring can provide a constant compression during backing layer adhesion process.

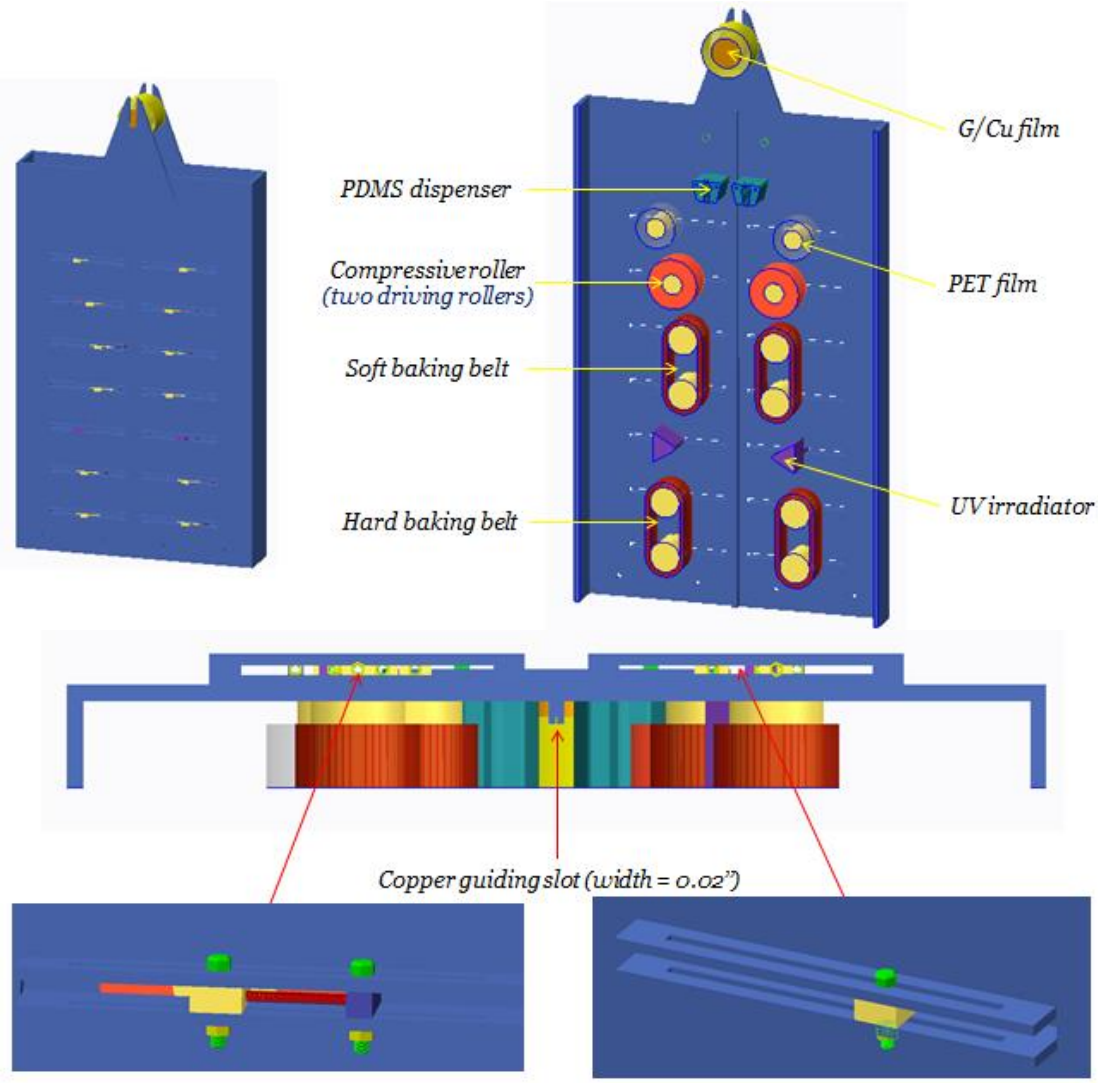

Figure 5.6 Backing layer adhesion unit

Large bending radius is used in the electrolysis unit to ensure smooth transition of the copper foil through the guiding slots from vertical section to horizontal section

(Figure 5.7). During the electrolysis, the copper foil connected to the side slots is used as the cathode and an inert platinum mesh is used as anode. The length of the horizontal section submerged in the aqueous sodium sulfate solution is adequate for complete graphene delamination.

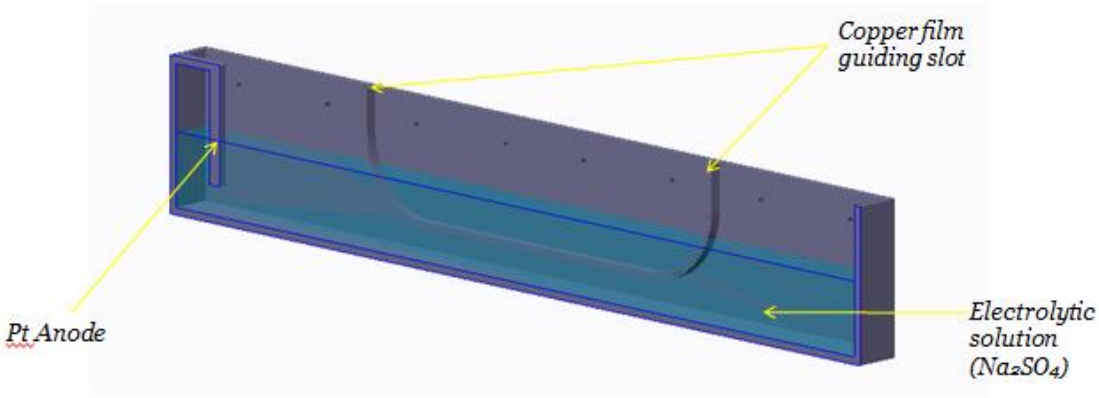

Figure 5.7 Electrolysis unit

Finally, the delaminated graphene on PDMS and plastic film are collected with two side rollers. The copper foil in the middle is also rolled back on a third roller for reuse. No guiding slot is used in this unit, and the three collection rollers are all driving rollers.

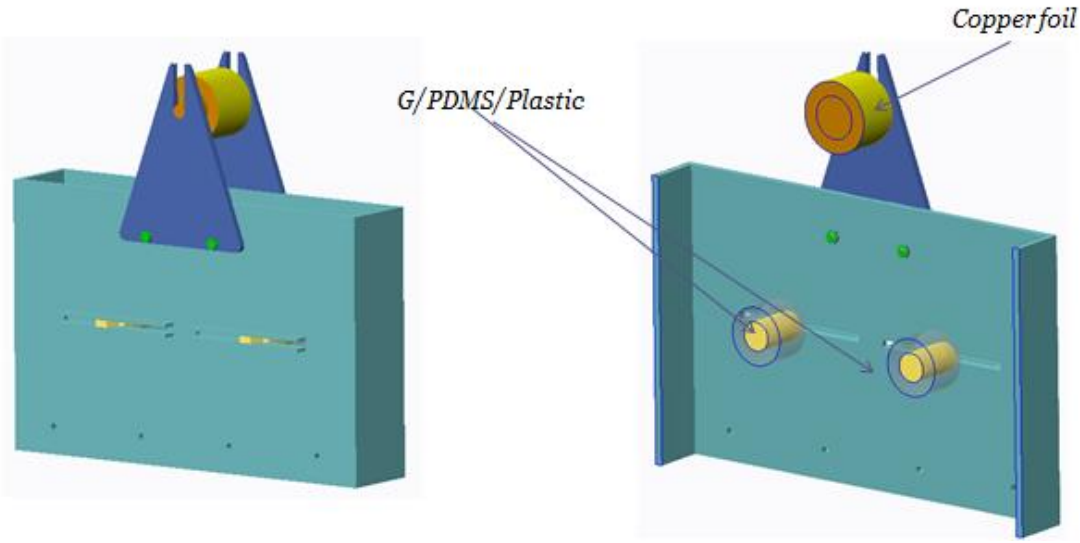

Figure 5.8 Collection unit

5.3 SUMMARY

A roll-to-roll graphene transfer machine is design to implement the proposed bilayer polymer support consisting of liquid PDMS and plastic film. Liquid PDMS precursor is dispensed between the graphene on copper foil and the plastic film. Two rollers are used to apply a uniform pressure so that a thin PDMS layer can be formed. A guiding slot is added to better align the copper foil with multiple rollers throughout the entire transfer process. Electrochemical delamination is used to separate graphene film from the copper foil instead of chemical etching. To avoid the prolonged curing time, photocurable PDMS is used, which requires a soft baking before UV radiation and a hard baking afterwards. Finally, a three-unit detachable machine is designed to achieve a clean and efficient double-sided roll-to-roll graphene transfer that is suitable for large-scale industrial fabrication of graphene-based electronics.

Chapter 6 Summary and Future Work

6.1 THESIS SUMMARY

Graphene-based devices, especially flexible transparent electrodes and ultrahigh-speed transistors, are rising to be promising candidates for post-silicon electronics. Chemical vapor deposition (CVD) is commonly used to synthesize large-area graphene films that are suitable for electronics fabrication. However, the quality of CVD graphene may be affected during the transfer process due to its brittleness as well as its stepped surface.

To achieve a high-quality, clean, and efficient graphene transfer, liquid PDMS precursor and a semi-rigid plastic film are used as the backing layer. Liquid PDMS can make a conformal contact with the relatively rough graphene surface and the plastic film can provide adequate support to the soft PDMS film during the graphene delamination process. Electrochemical delamination is used to gently separate graphene film from its growth substrate. Compared with wet etching, electrochemical delamination will not induce undesirable doping caused by metal etchant and the copper foils can be reused. The transferred graphene on PDMS/plastic film can be direct used for electronics fabrication. Moreover, graphene can be further transferred onto silicon wafer or other flexible substrates due to the extremely low work of adhesion between graphene and PDMS.

The intermediate PDMS layer between graphene and plastic film can act as a buffer layer to protect graphene-based electronics from external loads. From both analytical modeling and simulation, the strain isolation of PDMS is proven to be valid. In

addition, a higher Young's modulus of PDMS and greater PDMS layer thickness will lead to a better strain isolation effect.

Finally, a continuous roll-to-roll graphene transfer machine is designed to implement the proposed bilayer polymer support transfer with electrochemical delamination. Photocurable PDMS is proposed in this design to shorten the polymer curing time. This preliminary design could serve as a starting point for future designs of high-throughput graphene transfer equipment in the electronics industry.

List of the main contributions presented in this thesis:

1. A bilayer polymer support for graphene transfer consisting of liquid PDMS precursor and a semi-rigid plastic film. Together with electrochemical delamination, the proposed transfer process can achieve a high-quality, clean, and efficient graphene transfer.
2. The strain isolation effect of the intermediate PDMS layer between graphene and the plastic film has been verified by both analytical model and finite element analysis.
3. A prototype roll-to-roll graphene transfer machine is designed to implement the proposed transfer process that could serve as a starting point for large-scale industrial fabrication of graphene-based electronics.

6.2 FUTURE WORK

1. Field effect transistors and transparent electrodes can be made with transferred graphene by proposed the backing layer design to test the transfer quality.

2. In the finite element analysis of the strain isolation effect, graphene can be modeled with shell element instead of solid element, such that the graphene thickness effect can be considered in the simulation.

3. The size of graphene devices and the spacing between them can be studied in the finite element analysis. Based on the analytical model, wider spacing and a smaller device size will have a better strain isolation effect.

4. In light of the high price of photocurable PDMS, a roll-to-roll graphene transfer machine with traditional PDMS curing process need to be developed.

Bibliography

[1] Novoselov, Kostya S., et al. "Electric field effect in atomically thin carbon films." Science 306.5696 (2004): 666-669.

[2] Geim, Andre K., and Konstantin S. Novoselov. "The rise of graphene." Nature materials 6.3 (2007): 183-191.

[3] Lee, Changgu, et al. "Measurement of the elastic properties and intrinsic strength of monolayer graphene." science 321.5887 (2008): 385-388.

[4] Chen, Jian-Hao, et al. "Intrinsic and extrinsic performance limits of graphene devices on SiO2." Nature nanotechnology 3.4 (2008): 206-209.

[5] Watcharotone, Supinda, et al. "Graphene-silica composite thin films as transparent conductors." Nano Letters 7.7 (2007): 1888-1892.

[6] Lee, Jae-Ung, Duhee Yoon, and Hyeonsik Cheong. "Estimation of Young's modulus of graphene by Raman spectroscopy." Nano letters 12.9 (2012): 4444-4448.

[7] Zhang, Hao-Bin, et al. "Electrically conductive polyethylene terephthalate /graphene nanocomposites prepared by melt compounding." Polymer 51.5 (2010): 1191-1196.

[8] Jiang, Jin-Wu, Jian-Sheng Wang, and Baowen Li. "Young's modulus of graphene: a molecular dynamics study." Physical Review B 80.11 (2009): 113405.

[9] Lu, Qiang, and Rui Huang. "Nonlinear mechanics of single-atomic-layer graphene sheets." International Journal of Applied Mechanics 1.03 (2009): 443-467.

[10] Xiao, J. R., J. Staniszewski, and J. W. Gillespie Jr. "Fracture and progressive failure of defective graphene sheets and carbon nanotubes." Composite structures 88.4 (2009): 602-609.

[11] Bolotin, Kirill I., et al. "Ultrahigh electron mobility in suspended graphene." Solid State Communications 146.9 (2008): 351-355.

[12] Bae, Sukang, et al. "30 inch roll-based production of high-quality graphene films for flexible transparent electrodes." arXiv preprint arXiv:0912.5485 (2009).

[13] Kim, Keun Soo, et al. "Large-scale pattern growth of graphene films for stretchable transparent electrodes." Nature 457.7230 (2009): 706-710.

[14] Nair, R. R., et al. "Fine structure constant defines visual transparency of graphene." Science 320.5881 (2008): 1308-1308.

[15] Apell, S. Peter, G. W. Hanson, and C. Hägglund. "High optical absorption in graphene." arXiv preprint arXiv:1201.3071 (2012).

[16] Allen, Matthew J., Vincent C. Tung, and Richard B. Kaner. "Honeycomb carbon: a review of graphene." Chemical reviews 110.1 (2009): 132-145.

[17] Berger, Claire, et al. "Ultrathin epitaxial graphite: 2D electron gas properties and a route toward graphene-based nanoelectronics." The Journal of Physical Chemistry B 108.52 (2004): 19912-19916.

[18] Gao, M., et al. "Epitaxial growth and structural property of graphene on Pt (111)." Applied Physics Letters 98.3 (2011): 033101-033101.

[19] Sutter, Peter W., Jan-Ingo Flege, and Eli A. Sutter. "Epitaxial graphene on ruthenium." Nature materials 7.5 (2008): 406-411.

[20] Unarunotai, Sakulsuk, et al. "Layer-by-layer transfer of multiple, large area sheets of graphene grown in multilayer stacks on a single SiC wafer." ACS nano 4.10 (2010): 5591-5598.

[21] Li, Xuesong, et al. "Large-area synthesis of high-quality and uniform graphene films on copper foils." Science 324.5932 (2009): 1312-1314.

[22] Kumar, Ajay, and Chee Huei Lee. "Synthesis and biomedical applications of graphene: present and future trends." (2013).

[23] Juang, Zhen-Yu, et al. "Graphene synthesis by chemical vapor deposition and transfer by a roll-to-roll process." Carbon 48.11 (2010): 3169-3174.

[24] Reina, Alfonso, et al. "Large area, few-layer graphene films on arbitrary substrates by chemical vapor deposition." Nano letters 9.1 (2008): 30-35.

[25] Hesjedal, Thorsten. "Continuous roll-to-roll growth of graphene films by chemical vapor deposition." Applied Physics Letters 98.13 (2011): 133106-133106.

[26] Pham, Phi. "Transferring chemical vapor deposition grown graphene."

[27] Li, Xuesong, et al. "Transfer of large-area graphene films for high-performance transparent conductive electrodes." Nano letters 9.12 (2009): 4359-4363.

[28] Ren, Yujie, et al. "An improved method for transferring graphene grown by chemical vapor deposition." Nano 7.01 (2012).

[29] Pirkle, A., et al. "The effect of chemical residues on the physical and electrical properties of chemical vapor deposited graphene transferred to SiO_2." Applied Physics Letters 99.12 (2011): 122108-122108.

[30] Her, Michael, Ryan Beams, and Lukas Novotny. "Graphene transfer with reduced residue." Physics Letters A (2013).

[31] Minami, Tadatsugu. "Transparent conducting oxide semiconductors for transparent electrodes." Semiconductor Science and Technology 20.4 (2005): S35.

[32] Pang, Shuping, et al. "Graphene as transparent electrode material for organic electronics." Advanced Materials 23.25 (2011): 2779-2795.

[33] Wu, Junbo, et al. "Organic solar cells with solution-processed graphene transparent electrodes." Applied Physics Letters 92 (2008): 263302.

[34] Wu, Junbo, et al. "Organic light-emitting diodes on solution-processed graphene transparent electrodes." ACS nano 4.1 (2009): 43-48.

[35] Kim, Jin Young, et al. "Efficient tandem polymer solar cells fabricated by all-solution processing." Science 317.5835 (2007): 222-225.

[36] Chen, Jian-Hao, et al. "Intrinsic and extrinsic performance limits of graphene devices on SiO2." Nature nanotechnology 3.4 (2008): 206-209.

[37] Bae, Sukang, et al. "Roll-to-roll production of 30-inch graphene films for transparent electrodes." Nature nanotechnology 5.8 (2010): 574-578.

[38] De, Sukanta, and Jonathan N. Coleman. "Are there fundamental limitations on the sheet resistance and transmittance of thin graphene films?." Acs Nano 4.5 (2010): 2713-2720.

[39] Geim, Andre K. "Nobel lecture: random walk to graphene." Reviews of Modern Physics 83.3 (2011): 851.

[40] Liao, Lei, et al. "High-speed graphene transistors with a self-aligned nanowire gate." Nature 467.7313 (2010): 305-308.

[41] Lin, Yu-Ming, et al. "Operation of graphene transistors at gigahertz frequencies." Nano Letters 9.1 (2008): 422-426.

[42] Lin, Y-M., et al. "100-GHz transistors from wafer-scale epitaxial graphene." Science 327.5966 (2010): 662-662.

[43] Liu, Guanxiong, et al. "Graphene-Based Non-Boolean Logic Circuits." arXiv preprint arXiv:1308.2931 (2013).

[44] Reddy, Dharmendar, et al. "Graphene field-effect transistors." Journal of Physics D: Applied Physics 44.31 (2011): 313001.

[45] Ramon, M., et al. "3GHz Graphene Frequency Doubler on Quartz Operating Beyond the Transit Frequency." (2012): 1-1.

[46] Lin, Yu-Ming, et al. "Dual-Gate Graphene FETs With< formula formulatype=." Electron Device Letters, IEEE 31.1 (2010): 68-70.

[47] Kang, Junmo, et al. "Graphene transfer: key for applications." Nanoscale 4.18 (2012): 5527-5537.

[48] Morozov, S. V., et al. "Giant intrinsic carrier mobilities in graphene and its bilayer." Physical Review Letters 100.1 (2008): 016602.

[49] Meyer, Jannik C., et al. "The structure of suspended graphene sheets." Nature 446.7131 (2007): 60-63.

[50] Novoselov, K. S. A., et al. "Two-dimensional gas of massless Dirac fermions in graphene." nature 438.7065 (2005): 197-200.

[51] Lee, Youngbin, et al. "Wafer-scale synthesis and transfer of graphene films." Nano letters 10.2 (2010): 490-493.

[52] Wang, Yanjie, et al. "Scalable synthesis of graphene on patterned Ni and transfer." Electron Devices, IEEE Transactions on 57.12 (2010): 3472-3476.

[53] De Arco, L. Gomez, et al. "Synthesis, transfer, and devices of single-and few-layer graphene by chemical vapor deposition." Nanotechnology, IEEE Transactions on 8.2 (2009): 135-138.

[54] Reina, Alfonso, et al. "Growth of large-area single-and bi-layer graphene by controlled carbon precipitation on polycrystalline Ni surfaces." Nano Research 2.6 (2009): 509-516.

[55] Caldwell, Joshua D., et al. "Technique for the dry transfer of epitaxial graphene onto arbitrary substrates." ACS nano 4.2 (2010): 1108-1114.

[56] Jiao, Liying, et al. "Creation of nanostructures with poly (methyl methacrylate)-mediated nanotransfer printing." Journal of the American Chemical Society 130.38 (2008): 12612-12613.

[57] Reina, Alfonso, et al. "Transferring and identification of single-and few-layer graphene on arbitrary substrates." The Journal of Physical Chemistry C 112.46 (2008): 17741-17744.

[58] Gates, Byron D., et al. "New approaches to nanofabrication: molding, printing, and other techniques." Chemical reviews 105.4 (2005): 1171-1196.

[59] S. J. Clarson and J. A. Semlyen, Siloxane Polymers, Prentice Hall, Englewood Cliffs, NJ, 1993

[60] Kang, Seok Ju, et al. "Inking Elastomeric Stamps with Micro‐Patterned, Single Layer Graphene to Create High‐Performance OFETs." Advanced Materials 23.31 (2011): 3531-3535.

[61] Suganuma, Koichi, et al. "Fabrication of Transparent and Flexible Organic Field-Effect Transistors with Solution-Processed Graphene Source--Drain and Gate Electrodes." Applied physics express 4.2 (2011): 1603.

[62] Kim, Sung Min, et al. "Suspended few-layer graphene beam electromechanical switch with abrupt on-off characteristics and minimal leakage current." Applied Physics Letters 99 (2011): 023103.

[63] Song, Li, et al. "Transfer printing of graphene using gold film." ACS nano 3.6 (2009): 1353-1356.

[64] Lee, Yu-Ying, et al. "Top laminated graphene electrode in a semitransparent polymer solar cell by simultaneous thermal annealing/releasing method." ACS nano 5.8 (2011): 6564-6570.

[65] Chen, Xu-Dong, et al. "High-quality and efficient transfer of large-area graphene films onto different substrates." Carbon (2013).

[66] Suo, Zhigang. "Mechanics of stretchable electronics and soft machines." MRS bulletin 37.03 (2012): 218-225.

[67] Kim, Sung Hwan, et al. "Flexible, stretchable and implantable PDMS encapsulated cable for implantable medical device." Biomedical Engineering Letters 1.3 (2011): 199-203.

[68] Cheng, H., et al. "An analytical model of strain isolation for stretchable and flexible electronics." Applied Physics Letters 98.6 (2011): 061902-061902.

[69] Kim, Dae‐Hyeong, et al. "Ultrathin Silicon Circuits With Strain‐Isolation Layers and Mesh Layouts for High‐Performance Electronics on Fabric, Vinyl, Leather, and Paper." Advanced Materials 21.36 (2009): 3703-3707.

[70] Kim, Rak-Hwan, et al. "Waterproof AlInGaP optoelectronics on stretchable substrates with applications in biomedicine and robotics." Nature materials 9.11 (2010): 929-937.

[71] Kim, Dae-Hyeong, et al. "Materials for multifunctional balloon catheters with capabilities in cardiac electrophysiological mapping and ablation therapy." Nature materials 10.4 (2011): 316-323.

[72] Kim, Dae‐Hyeong, et al. "Optimized structural designs for stretchable silicon integrated circuits." Small 5.24 (2009): 2841-2847.

[73] Kim, Dae‐Hyeong, et al. "Stretchable, curvilinear electronics based on inorganic materials." Advanced Materials 22.19 (2010): 2108-2124.

[74] Ohno, Yasuhide, et al. "Electrolyte-gated graphene field-effect transistors for detecting pH and protein adsorption." Nano Letters 9.9 (2009): 3318-3322.

[75] Geim, Andre Konstantin. "Graphene: status and prospects." science 324.5934 (2009): 1530-1534.

[76] Liang, Xuelei, et al. "Toward clean and crackless transfer of graphene." ACS nano 5.11 (2011): 9144-9153.

[77] Kang, Junmo, et al. "Efficient transfer of large-area graphene films onto rigid substrates by hot pressing." ACS nano 6.6 (2012): 5360-5365.

[78] Wang, Yu, et al. "Electrochemical delamination of CVD-grown graphene film: toward the recyclable use of copper catalyst." ACS nano 5.12 (2011): 9927-9933.

[79] Gao, Libo, et al. "Repeated growth and bubbling transfer of graphene with millimetre-size single-crystal grains using platinum." Nature Communications 3 (2012): 699.

[80] de la Rosa, César J. Lockhart, et al. "Frame assisted H 2 O electrolysis induced H 2 bubbling transfer of large area graphene grown by chemical vapor deposition on Cu." Applied Physics Letters 102.2 (2013): 022101-022101.

[81] Khang, Dahl-Young, et al. "A stretchable form of single-crystal silicon for high-performance electronics on rubber substrates." Science 311.5758 (2006): 208-212.

[82] Sun, Jeong-Yun, et al. "Inorganic islands on a highly stretchable polyimide substrate." Journal of Materials Research 24.11 (2009): 3338-3342.

[83] Sun, Jeong-Yun, et al. "Debonding and fracture of ceramic islands on polymer substrates." Journal of Applied Physics 111.1 (2012): 013517-013517.

[84] Sun, Jeong-Yun, et al. "Islands stretch test for measuring the interfacial fracture energy between a hard film and a soft substrate." Journal of Applied Physics 113 (2013): 223702.

[85] Rafat, Marjan, et al. "Fabrication of reversibly adhesive fluidic devices using magnetism." Lab Chip 9.20 (2009): 3016-3019.

[86] Kobayashi, Toshiyuki, et al. "Production of a 100-m-long high-quality graphene transparent conductive film by roll-to-roll chemical vapor deposition and transfer process." Applied Physics Letters 102.2 (2013): 023112-023112.

[87] Singha, K. (2012). A Review on Coating & Lamination in Textiles: Processes and Applications. American Journal of Polymer Science, 2(3), 39-49.

[88] Lötters, J. C., et al. "Polydimethylsiloxane, a photocurable rubberelastic polymer used as spring material in micromechanical sensors." Microsystem technologies 3.2 (1997): 64-67.

[89] Choi, Kyung M., and John A. Rogers. "A photocurable poly (dimethylsiloxane) chemistry designed for soft lithographic molding and printing in the nanometer regime." Journal of the American Chemical Society 125.14 (2003): 4060-4061.

[90] Tsougeni, Katerina, Angeliki Tserepi, and Evangelos Gogolides. "Photosensitive poly (dimethylsiloxane) materials for microfluidic applications." Microelectronic engineering 84.5 (2007): 1104-1108.